Available online at www.sciencedirect.com
ScienceDirect
Geochimica et Cosmochimica Acta 74 (2010) 3621–3641
Geochimica et Cosmochimica Acta
www.elsevier.com/locate/gca

Lithium isotopes in Guatemalan and Franciscan HP–LT rocks: Insights into the role of sediment-derived fluids during subduction

Kyla K. Simons [a,*], George E. Harlow [b], Hannes K. Brueckner [a,c], Steven L. Goldstein [a], Sorena S. Sorensen [d], N. Gary Hemming [a,c], Charles H. Langmuir [e]

[a] Lamont-Doherty Earth Observatory and Department of Earth and Environmental Sciences, Columbia University, Palisades, NY 10964, USA
[b] Department of Earth and Planetary Sciences, American Museum of Natural History, New York, NY 10024, USA
[c] School of Earth and Environmental Sciences, Queens College, CUNY, Flushing, NY 11367, USA
[d] Department of Mineral Sciences, Smithsonian Institution, Washington, DC 37012, USA
[e] Department of Earth and Planetary Science, Harvard University, Cambridge, MA 02138, USA

Received 6 March 2009; accepted in revised form 19 February 2010; available online 6 March 2010

Abstract

High-pressure, low-temperature (HP–LT) rocks from a Cretaceous age subduction complex occur as tectonic blocks in serpentinite mélange along the Motagua Fault (MF) in central Guatemala. Eclogite and jadeitite among these are characterized by trace element patterns with enrichments in fluid mobile elements, similar to arc lavas. Eclogite is recrystallized from MORB-like altered oceanic crust, presumably at the boundary between the down-going plate and overlying mantle wedge. Eclogite geochemistry, mineralogy and petrography suggest a two step petrogenesis of (1) dehydration during prograde metamorphism at low temperatures (<500 °C) followed by (2) partial rehydration/fertilization at even lower T during exhumation. In contrast, Guatemalan jadeitites are crystallized directly from low-T aqueous fluid as veins in serpentinizing mantle during both subduction and exhumation. The overall chemistry and mineralogy of Guatemalan eclogites are similar to those from the Franciscan Complex, California, implying similar P–T–x paths.

Li concentrations ($\leqslant$90 ppm) in mineral separates and whole rocks (WR) from Guatemalan and Franciscan HP–LT rocks are significantly higher than MORB (4–6 ppm), but similar to HP–LT rocks globally. Li isotopic compositions range from $-5‰$ to $+5‰$ for Guatemalan HP–LT rocks, and $-4‰$ to $+1‰$ for Franciscan eclogites, overlapping previous findings for other HP–LT suites. The combination of Li concentrations greater than MORB, and Li isotopic values lighter than MORB are inconsistent with a simple dehydration model. We prefer a model in which Li systematics in Guatemalan and Franciscan eclogites reflect reequilibration with subduction fluids during exhumation. Roughly 5–10% of the Li in these fluids is derived from sediments.

Model results predict that the dehydrated bulk ocean crust is isotopically lighter ($\delta^7Li \leqslant +1 \pm 3‰$) than the depleted mantle ($\sim+3.5 \pm 0.5‰$), while the mantle wedge beneath the arc is the isotopic complement of the bulk crust. A subduction fluid with an AOC–GLOSS composition over the full range of model temperatures (50–600 °C) gives an average fluid δ^7Li ($\sim+7 \pm 5‰$ 1σ) that is isotopically heavier than the depleted mantle. If the lowest temperature steps are excluded (50–260 °C) as too cold to participate in circulation of the mantle wedge, then the average subduction fluid ($\delta^7Li = +4 \pm 2.3‰$ 1σ, is indistinguishable from depleted mantle. Because of the relatively compatible nature of Li in metamorphic minerals, the most altered part of the crust (uppermost extrusives), may retain a Li isotopic signature ($\sim+5 \pm 3‰$) heavier than the bulk crust. The range of Li isotopic values for OIB, IAB and MORB overlap, making it is difficult to resolve which of these components may contribute to the recycled component in the mantle using δ^7Li alone.

* Corresponding author. Present address: RSMAS, University of Miami, Miami, FL 33149, USA. Tel.: +1 917 714 6885.
E-mail address: ksimons@rsmas.miami.edu (K.K. Simons).

0016-7037/$ - see front matter © 2010 Elsevier Ltd. All rights reserved.
doi:10.1016/j.gca.2010.02.033

1. INTRODUCTION

Earlier work on lithium (Li) concentrations and isotopic compositions focused on its use as a tracer for crustal recycling (e.g., Elliott et al., 2004). However, the discovery of sometimes significant δ^7Li disequilibrium inter- and intra-mineral in some mantle xenoliths, granulite xenoliths and ophiolites has shifted that focus to processes such as melt-rock interaction and diffusion (e.g., Ludstrom et al., 2005; Tang et al., 2007; Rudnick and Ionov, 2007; Jeffcoate et al., 2007; Teng et al., 2008). Several recent studies and experiments have shown that kinetic fractionation of Li via diffusion can be effective in generating Li isotopic variability at high temperatures (Richter et al., 2003; Ludstrom et al., 2005; Teng et al., 2006). These experiments, which show ^{6}Li diffusing up to ~3% faster than ^{7}Li (Richter et al., 2003), have been used to support observations of δ^7Li disequilibrium measured in xenoliths from San Carlos (Jeffcoate et al., 2007), eastern Russia (Rudnick and Ionov, 2007), nakhlite meteorites (Beck et al., 2006) and from the Trinity Ophiolite (Ludstrom et al., 2005). However, Ionov and Seitz (2008) noted that δ^7Li inter-mineral disequilibria in xenoliths from their study and the literature did not appear to be linked to tectonic setting, or chemical composition of the xenolith, but rather to the type of volcanic rock hosting the xenolith. In other words, δ^7Li tended to be in equilibrium in xenoliths hosted by rocks that cooled almost instantaneously, like pyroclastic rocks, while δ^7Li disequilibrium was common in xenoliths hosted in massive basalts, which cooled slowly post-eruption, providing time for Li to diffuse between the xenolith and host lava. This observation suggests that perhaps some of the δ^7Li disequilibrium measured to date is generated during post-eruptive processes, rather than exclusively in the mantle. Li isotopes measured in quick quenching mid-ocean ridge basalt (MORB) glasses (e.g., Elliott et al., 2006; Tomascak et al., 2008; Simons et al., 2008) appear to avoid a lot of theses post-eruptive complexities, with good correlations between δ^7Li other geochemical tracers for data sets with high precision (better than $\pm$0.4‰). However, the recognition that Li isotopes are susceptible to high-T kinetic fraction under certain circumstances has lead to some skeptism about the usefulness of Li isotopes as a tracer for crustal recycling.

Most studies of δ^7Li prior to the wide-spread recognition of Li diffusion, focused on the volcanic output of Li associated with MORB (Chan et al., 1992, 2002a; Moriguti and Nakamura, 1998a; Elliott et al., 2006; Nishio et al., 2007; Tomascak et al., 2008), ocean island basalts (e.g., Chan and Frey, 2003; Ryan and Kyle, 2004; Nishio et al., 2005; Chan et al., 2006b, 2009) and subduction zones (e.g., Moriguti and Nakamura, 1998a; Benton and Tera, 2000; Tomascak et al., 2000, 2002; Chan et al., 2001, 2002a; Benton et al., 2004; Leeman et al., 2004; Agostini et al., 2008). While several studies have addressed the input of Li at subduction zones in the form of altered oceanic crust (e.g., Seyfried et al., 1984; Ryan and Langmuir, 1987; Chan and Edmond, 1988; Chan et al., 1992, 2002b; Decitre et al., 2002) and sediments (Chan et al., 1994, 2006a; You et al., 1995; You and Chan, 1996; Chan and Kastner, 2000; Bouman et al., 2004), more work is necessary to better understand the distribution of δ^7Li through the ocean crust. Surprisingly little is known about the behavior and budget of Li within the subduction zone itself, and there are few published measurements of δ^7Li in exhumed high pressure subduction mélanges (e.g., Zack et al., 2003; Marschall et al., 2007b). Furthermore, while a heavy δ^7Li signature in the overlying mantle wedge (and conversely a light δ^7Li slab) has been predicted and/or observed by some (e.g., Zack et al., 2003; Elliott et al., 2004; Bouman et al., 2004; Brooker et al., 2004), the majority of data on δ^7Li in convergent margins continues to come indirectly from measurements of arc lavas, with most values overlapping those of MORB and ocean island basalt (OIB). Thus in order to evaluate the usefulness of δ^7Li as a tracer of subduction processes, it is necessary to collect more data on high-P, low-T rocks to assess how Li behaves during dehydration, and to determine the role of diffusion during subduction.

We report new high precision measurements of Li abundances and isotopes on blocks of eclogite, jadeitite and amphibolite from Guatemala and California, which provide constraints on the Li systematics of the down-going slab, mantle wedge, and the range of δ^7Li subducted to the deep mantle.

1.1. Tectonic Setting

The Motagua fault (MF) is an active left-lateral strike-slip fault that marks the northern boundary of the Caribbean plate in Central America (Fig. 1). It is the central and most active fault among three parallel faults that define the Guatemala suture zone (GSZ). Serpentinite-matrix mélanges exist on both sides of the MF, for over 100 km on the north side and some 50 km on the south. Meter-size blocks of eclogite, jadeitite, albitite, amphibolite and/or blueschist are found in dismembered outcrops and as boulders in stream beds traversing these serpentinite–matrix mélanges (e.g., Harlow et al., 2004). Northern and southern belts can be further divided on the basis of mineralogical and petrographic differences, and estimated equilibration P–T conditions. The northern belt represents a hotter subduction geotherm (7–10 °C/km; ⩽500–600 °C at ~2 GPa) and consists of amphibolite, amphibolitized eclogite, jadeitite and albitite, while the southern belt represents a very cold geotherm (~5 °C/km;) with lawsonite eclogite, jadeitite, blueschist and mica schist (Tsujimori et al., 2004, 2006a,b). Eclogites from both belts give Sm–Nd mineral isochron ages of ~130–140 Ma (Brueckner et al., 2005), but differ in ^{40}Ar/^{39}Ar geochronology of phengite and amphibole, suggesting that the northern side was reset by a later metamorphic event at ~65–77 Ma (Harlow et al., 2004; Brueckner et al., 2007). This event was therefore warm enough to reset the Ar systematics and overprint the northern eclogites to amphibolite facies, but not hot or wet enough to transform (retrogress) the jadeitites or reset the Sm–Nd systematics of the eclogites. Therefore southern rocks are the best representatives of the coldest and deepest P–T conditions during subduction.

The prograde mineral assemblage for Guatemala's southern eclogites is composed mainly of Omphacite

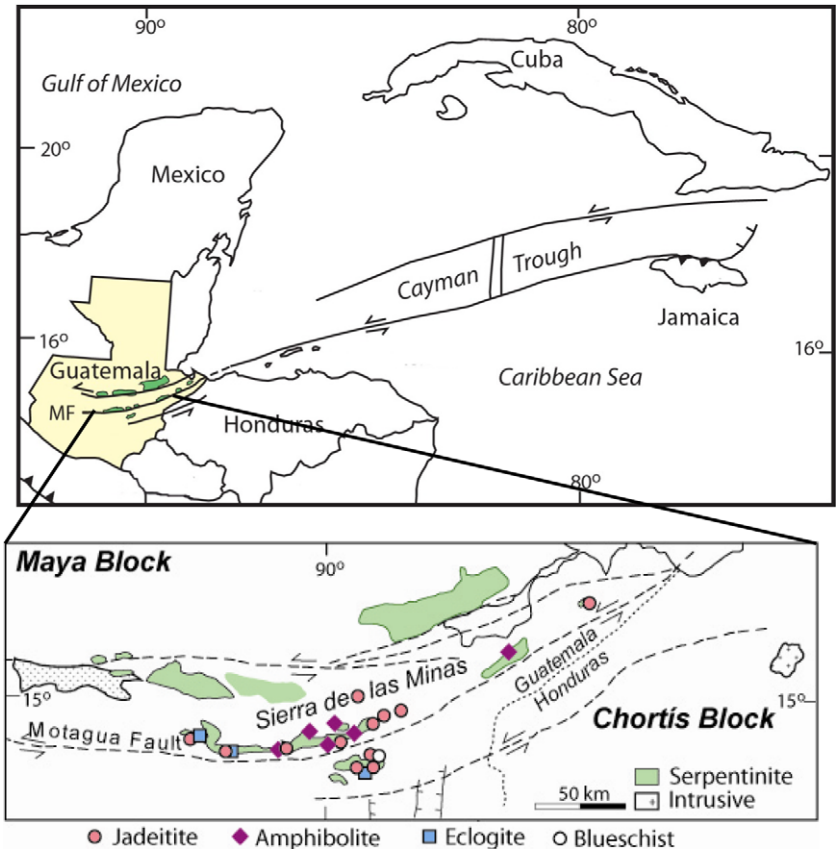

Fig. 1. Map of the Caribbean showing the Guatemala suture zone with its three major strike-slip faults, the Motagua Fault (MF) being the central of these and the focus of this study. The inset shows a closer view of the MF and the distribution of HP–LT rock types within the serpentinite bodies (in green) north and south of the MF. (For interpretation of the references to color in this figure legend, the reader is referred to the web version of this article.)

(Omp) + Garnet (Grt) (50–80%) + Lawsonite (Lws) + Rutile (Rt) + Quartz (Qtz) ± Chlorite (Chl) ± Phengite (Phe) ± Glaucophane (Gln) ± Ilmenite (Ilm), suggesting that deformation of eclogites initiated at $T = \sim 300$ °C and $P > 1.1$ GPa and continued to $T = \sim 470$ °C and $P = \sim 2.5$ GPa (Tsujimori et al., 2006a). A cold, wet blueschist facies retrograde recrystallization is suggested by the surviving mineral assemblage (Gln + Lws + Chl + Phe + Titanite (Ttn) + Qtz ± rare Ab). Retrograde deformation most likely occurred at shallower levels in the subduction system upon exhumation, with estimates of ~1.8 GPa and ~400 °C, and perhaps as low as $P = \sim 0.7$ GPa and $T < \sim 300$ °C (Tsujimori et al., 2005). Retrograde metamorphism may also be responsible for the hydration of peridotite to serpentinite (antigorite) associated with the high-pressure rocks in the mélange. The presence of antigorite suggests a temperature in the reacting peridotite greater than at least 350 °C, perhaps closer to 400 °C (Evans, 2004). Metasomatic rocks, such as jadeitite and omphacitite, are also likely to be synchronous with the retrograde blueschist facies stage, precipitating from subduction fluids over a range of P (0.6–1.0 GPa) and T (300–400 °C; Harlow, 1994; Harlow et al., 2003; Harlow and Sorensen, 2005; Tsujimori et al., 2006a). Mineralogy, petrography, and alteration of Guatemalan HP–LT rocks are discussed further in Appendix A.

The petrology and mineralogy of Franciscan eclogites are similar to those of Guatemala. Franciscan eclogites analyzed in this study are from rock powders, however, samples are described in detail in Sorensen et al. (1997). Eclogite blocks come from different areas within the Franciscan (e.g., near Mt. Hamilton in the Diablo Range, Central Melange Belt at Healdsburg and Ring Mt. Tiburon Peninsula). A generalized eclogite block mineralogy consists of Grt + Omp + Gln (±Act, barroisite) + Phe + Rt + Chl + Ttn ± Ep ± Qtz ± Zir (Oh and Liou, 1990; Sorensen et al., 1997). Coarse-grained blocks have been variably overprinted by blueschist facies minerals like Chl + Phe and minor blue amphibole (Page et al., 2003). Others have metamorphic rinds of Act ± talc ± Chl formed during metasomatic reactions with serpentinizing peridotite (Oh and Liou, 1990). P–T estimates from Page et al. (2003) for Healdsburg eclogite blocks (e.g., GL-14) give peak prograde conditions of 400–475 °C and 1.1–1.4 GPa, which are similar to those for the Ward Creek eclogite (480–540 °C and 1.0–1.15 GPa) from Oh and Liou (1990). Giaramita and Sorensen (1994) estimate similar P (~0.9–1.5 GPa) for blocks from the Tiburon Peninsula and Mt. Hamilton

(T90-1b, T90-5, MH90-1), but at slightly higher T ~650 ± 55 °C. Overall, the similarities in petrology, mineralogy and P–T conditions between Franciscan and Guatemalan eclogites suggest similar P–T–x paths, and therefore rocks from these two locals will be directly compared in this study.

Jadeitites from four locations outside of Guatemala have been measured to compare to those from Guatemala. These include Myanmar (MJE00-CJ1 and MJE02-3-15), Kazakhstan (AMNH102029), Ketchpel River, Polar Urals (AMNH104278) and Kotaki-gawa, Itoi-gawa Japan (OKJ00-4-1). Jadeitites from all locations share similar mineralogy, petrography and P–T conditions to those described above for Guatemala (Harlow and Sorensen, 2005; Sorensen et al., 2006; Harlow et al., 2007). All localities involved subduction of oceanic crust, followed by a collisional event involving at least one continental block.

1.2. Physical model

Previous studies (e.g., Tsujimori et al., 2005; Sorensen et al., 2006; Harlow et al., 2007) have established that these HP–LT assemblages form as the result of complex multistage processes during subduction and exhumation. Guatemalan eclogites and many other HP–LT rocks, can be modeled most simply by a two-stage process of prograde dehydration and retrograde hydration. Stage one involves normal subduction, dehydration and metamorphism of the oceanic plate which leads to the transformation of basaltic crust into blueschist and eclogite. Stage two involves exhumation of the blocks and serpentinized matrix and geochemical overprinting (fertilization) by subduction fluids channeled along the shear zone as the collision proceeds.

The collision of the Maya and Chortís continental blocks at approximately 130 Ma, initiated a change in regional tectonics that eventually lead to the formation of the GSZ, and the exhumation of the HP–LT rocks presented in this paper. It is likely that the change in geometry of subduction, as a consequence of the collision, enabled blocks from the top of the metamorphosed slab to be transferred (sheared) into the shear zone mélange that lies between the down-going slab and overlying mantle wedge. Various authors have suggested that development of a shear zone in the hanging wall along the interface with the down-going slab is likely a zone of focused fluid flow where rocks become geochemical hybrids with strong fluid overprints (e.g., King et al., 2006; Bebout et al., 2007). Geochemical hybridization results from both mechanical mixing, as well as metasomatic fluid flow, which enhances the stability of key metamorphic and metasomatic phases during subduction (Bebout and Barton, 1993, 2002; King et al., 2006). Hybridization is supported by studies of O–H–N isotopes which become pervasively homogenized in these mélange zones along with extensive redistribution of trace elements (Bebout, 1991, 1997; Bebout and Barton, 1993, 2002). These fluids may be generated locally from dehydration of the slab directly below the subduction channel (vertical fluid flow), or fluids may travel along the channel from deeper in the system. A strong fluid overprinting, as is evident in the geochemistry of Guatemalan and Franciscan eclogites and blueschists, means that although these blocks were originally part of the down-going slab, upon collision–exhumation they were infiltrated and recrystallized in the presence of fluids in the subduction channel at moderate to shallow depths (e.g., <75 km). Similar fluid overprinting during exhumation has been recognized for other eclogite localities such as Trescolmen (Zack et al., 2001) and Syros (Marschall et al., 2006), and was suggested as a mechanism to explain B enrichments and isotopes for lawsonite eclogites from the Central Pontides area of Turkey (Altherr et al., 2004). Vein crystallizations such as jadeitite are even more useful in constraining fluid compositions, as they have no protolith and are formed by direct precipitation of subduction derived fluids permeating the mélange and fragments of the mantle wedge. Thus Guatemalan eclogites, blueschists and jadeitites may be excellent recorders of the composition of subduction fluids present at the interface between the down-going slab and overlying mantle wedge. Given the similarities in overall P–T conditions, mineralogy and geochemistry between Franciscan and Guatemalan eclogites, a similar two-stage process is assumed for the Franciscan HP–LT assemblages. We will examine Li concentrations and isotopic compositions in the context of this two-stage model for the origin of HP–LT rocks.

2. METHODS

2.1. Lithium isotopes

Our chemistry and column procedure follows Tomascak et al. (1999a), with some modifications. This chemistry is based on the efficient separation of Li from other interfering elements (particularly Na) using a cation exchange resin and a mixture of nitric acid and methanol to achieve maximum separation. The method was first developed by Strelow et al. (1974) and has been the basis of the chemistry of many other groups (e.g., Moriguti and Nakamura, 1998b; Tomascak et al., 1999a; Nishio and Nakai, 2002; Pistiner and Henderson, 2003; Ryan and Kyle, 2004). We have modified the original column procedure of Tomascak et al. (1999a) to include an optional second column, which serves to remove any organics or resin that leaked through the first column, and further separates Na from Li if necessary.

Samples were run on a VG Axiom Multi-Collector ICP-MS, and were introduced via an all Teflon PFA spray chamber, a 20 µl/min nebulizer and a peristaltic pump, to ensure a consistent flow of sample into the plasma. The advantages of the Axiom-PFA set-up, compared to the standard ICP-MS desolvating nebulizer (e.g., Aridus) method, are (1) stability, (2) very efficient washout between samples and (3) minimal matrix effects. In-run precision for block averages is between 0.03‰ and 0.07‰ (2σ). The external precision was determined by calculating the average and 2σ standard deviation of multiple runs of standards IRMM-016, UMD-1 and L-SVEC, as well as natural standards JB2 and seawater, over the course of 13 months. External precision is ±0.4‰ (2σ) or better for isotopic analyses, and ±7% for Li concentration (2σ). This method pro-

duced a fast, efficient washout with little to no drift for the average run. Thus we make no corrections to the measured ratios apart from bracketing of standards. Matrix tests using the Axiom-PFA set-up resulted in no deviations of $^{7}Li/^{6}Li$ over the range of Na/Li investigated ($\leqslant$50; Fig. 2). This result is similar to other Li isotopic studies using ICP-MS instruments without desolvating membranes (e.g., Kosler et al., 2001; Bryant et al., 2003; Rosner et al., 2007), and is an improvement over the matrix problems reported for methods that include a desolvating membrane (e.g., Jeffcoate et al., 2004; Nishio and Nakai, 2002; Fig. 2). A more detailed description of the methods used here are available in Appendix B.

2.2. Trace elements

Trace element compositions were measured via ICP-MS at Harvard University, and were digested and run by two separate methods. The first method used a HNO_3–HF digestion, the second a $LiBO_2$ fusion. The HNO_3–HF method employed an overnight digestion in a picotrace dissolution unit, using 2 mL of 8 N HNO_3 and 0.5 mL of HF at 150 °C and then evaporated to dryness. To ensure complete dissolution, there was a second digestion step using 2 mL of 8 N HNO_3 at 150 °C overnight and then evaporated to dryness. Dried samples were re-dissolved in 4 mL of 4 N HNO_3 and transferred to HDPE bottles with 50 g of Internal Standard solution containing 50 ppb Ge, 25 ppb Rh, In, 25 ppb Tm and 25 ppb Bi, and diluted with de-ionized water to 1:5000 the original sample weight. The second method used, sample digestion by fusion, gives complete recovery of all trace elements by ensuring that all phases are digested. This second method was necessary as the HNO_3–HF digestion did not completely break down all of the zircon, apatite and ferroglaucophane in some of the Guatemalan eclogite whole rocks. $LiBO_2$ flux is combined with the sample to lower the melting point of the powder or rock chips. Samples were then re-dissolved in HNO_3 and used the same internal standard solution from the previous HNO_3–HF digestion for analysis on the ICP-MS. The fusion method is similar to the one described by Ramsey et al. (2005). Trace element concentrations affected by incomplete digestion in the HNO_3–HF method (e.g., Zr, Hf, P), were completely recovered by the fusion method. All other trace elements not affected by incomplete digestion are reproducible within 7% between the two methods.

Trace element compositions were measured using a Thermo Xseries. Within an ICP-MS run, each sample was measured twice to allow an estimate of in-run uncertainty. Standard K1919 was use to monitor instrument drift during each run. Raw data were first blank-corrected, then drift-corrected using K1919 and Internal Standard elements. The reproducibility of replicate analyses is generally better than 2% for the REE and elements such as Sc, V, Cr, Sr, Y, Zr, Nb and U, and better than 5% for the others (Cs, Rb, Ba, Th, Ta, Pb, Hf).

3. RESULTS

3.1. Guatemalan and Franciscan trace elements

A full suite of trace elements was measured in Guatemalan eclogites and jadeitites, and Franciscan eclogites. Representative trace element patterns are shown in Fig. 3, trace element data are reported in Appendix C, and Li data are reported in Tables 1 and 2.

Relative to MORB, Guatemalan eclogites and jadeitites are strongly enriched in fluid mobile trace elements (Cs, Rb, Ba, Pb, and Li), and moderately enriched in Th and U. Concentrations of HFSE (Nb, Ta, Zr, Hf) and HREE are within ~20% of the reference N-MORB (Sun and McDonough, 1989). Trace element patterns for the jadeitites are broadly similar to those of the eclogites, but with higher concentrations of Pb, U and Ba, and lower concentrations of REE (Fig. 3). Both eclogites and jadeitites have flat to slightly LREE-enriched trace element patterns compared to MORB, and with the exception of Eu, REE are always the most depleted trace elements in the jadeitites (~0.3× MORB). Franciscan eclogites share similar trace element patterns with their Guatemalan counterparts, with slightly

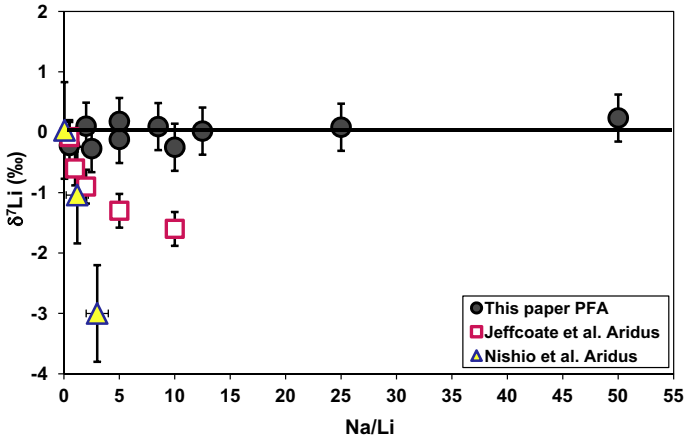

Fig. 2. Plot of Na/Li vs. $\delta^{7}Li$ to illustrate Na matrix effects. Unknowns are L-SVEC doped with varying amounts of Na. Unknowns run with the PFA are a compilation of 3 different days. Only samples introduced with the PFA were free from Na matrix effects over the Na/Li range tested. Sources for other data plotted are Jeffcoate et al. (2004) and Nishio and Nakai (2002).

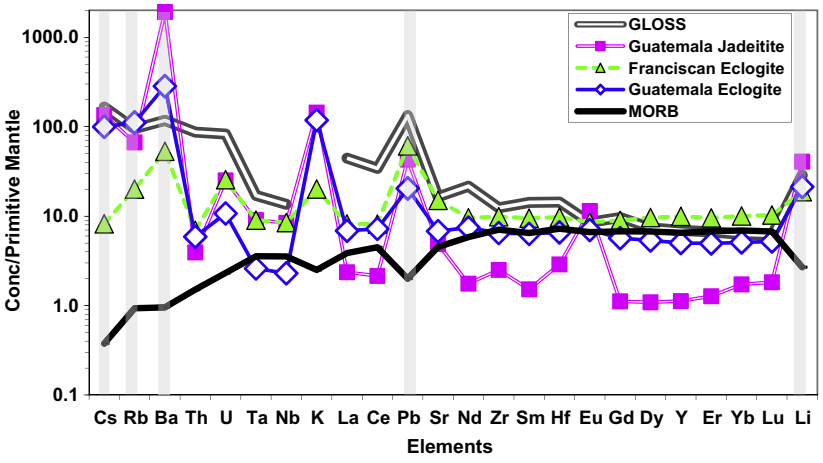

Fig. 3. Trace element diagram where concentrations are normalized to the Primitive Mantle of McDonough and Sun (1995). Elements are organized from right to left in order of increasing in compatibility during anhydrous peridotite melting. Plotted are whole rock averages of Guatemalan eclogite (southern) and jadeitite and Franciscan eclogite. The greatest enrichments (relative to N-MORB) are for the most fluid mobile elements (highlighted in grey). Guatemalan and Franciscan eclogites also show similarities to the pattern of Global Subducted Sediment (GLOSS) from Plank and Langmuir (1998). The reference N-MORB pattern of Sun and McDonough (1989) is plotted for comparison.

less enrichment in the most incompatible elements (Rb, Ba and Cs), and higher concentrations of REE, with flat to slight LREE-enriched patterns (Fig. 3). Complete discussion of the origin of these rocks is beyond the scope of this paper, however, existing work on major elements (Sorensen et al., 1997) and radiogenic isotopes (Nelson, 1991, 1995; Brueckner et al., 2005; Simons, 2008), together with trace element data from Sorensen et al. (1997) and new trace element data presented here, support a MORB protolith for these HP–LT eclogites.

3.2. Distribution of Li and Li isotopic compositions

3.2.1. Guatemala and the Franciscan

Almost all phases investigated in Guatemalan rocks have moderate to high Li concentrations (Table 1, Fig. 4). Overall, jadeite, omphacite and phengite have the highest Li concentrations ($\leqslant$90 ppm), with garnet and a clinopyroxene separate in serpentinite having the lowest ($\sim$0.5 ppm). Measured and calculated whole rock values for Guatemalan eclogites average 34.0 ± 2.5 ppm 1σ. Concentrations of Li in Franciscan rocks are also high, with whole rock values averaging 30.0 ± 6.5 ppm 1σ (Table 2). These Li concentrations for Guatemalan and Franciscan rocks are comparable to, but on average higher than, other subduction related HP rocks from Trescolmen (Zack et al., 2003), China, Greece, Germany, Norway and other locations in the Alps (Marschall et al., 2007b).

High Li concentrations in Guatemalan and Franciscan rocks are not surprising as most low-T subduction related eclogites have higher Li concentrations than their high-T equivalents. Woodland et al.'s (2002) study of Li (whole rock and separates) in eclogites and garnet clinopyroxenites from around the world found that Li is preferentially incorporated into eclogite minerals in the order clinopyroxene > phengite > garnet, and that when present, glaucophane had Li concentrations comparable to clinopyroxene. This sequence is similar to the findings of Marschall et al. (2006) and is the same mineral order found for Guatemalan separates. Woodland et al. (2002) also found that metabasites from HP–LT ($T < 700$ °C) terrains consistently had higher Li concentrations (14 ± 22 ppm) than high-T eclogites (880–1370 °C) from kimberlites and mantle xenoliths (1.2 ± 4.5 ppm). Taken together, these data show that high Li concentrations in low-T eclogites are a world-wide phenomenon. Li concentrations in HP–LT rocks may therefore play an important role in understanding the fluid exchange processes that occur in subduction zones.

In contrast to the large range of Li concentrations in mineral separates from Guatemala, the range of isotope ratios is small (Table 1, Fig. 4). The total isotopic range of δ^7Li for all HP–LT Guatemalan rocks in this study is $\sim$10‰, with a mean of -0.1 ± 4.5‰ 2σ There is no correlation between Li concentration and δ^7Li (Fig. 4). The average (measured and calculated) Guatemalan whole rock jadeitite ($\delta^7\text{Li} = +0.6 \pm 2.0$‰ 1σ, $n = 4$) is only slightly heavier than the average whole rock eclogite ($\delta^7\text{Li} = -0.5 \pm 1.8$‰ 1σ, $n = 6$), although the averages do overlap. The average δ^7Li for Franciscan whole rock eclogite ($n = 4$) is -2.1 ± 2.3‰ 1σ, which overlaps with published values (-1‰ to $+2$‰; Penniston-Dorland et al., 2008). Franciscan eclogites also shows no correlation between isotopes and concentration (Table 2).

3.2.2. Global jadeitites

Jadeitites ($n = 5$) from four other locations (Myanmar, Kazakhstan, Polar Urals, Japan) were measured for Li concentrations and δ^7Li. Concentrations and isotopes overlap the range of Guatemalan and Franciscan HP–LT rocks reported in this study, however, Li concentrations in individual jadeitites vary by approximately a factor of five (Table 2). Jadeitites from Myanmar have the highest Li concentra-

Table 1
Lithium concentrations and δ^7Li for mineral separates and whole rocks for Guatemalan HP–LT rocks.

Sample	Location	Li (ppm)	δ^7Li
Eclogites			
MVE04-7-2 omphacite	S	45.0	−1.48
MVE04-7-2 omphacite replicate			−1.52
MVE02-14-6 omphacite	S	48.0	−3.79
MVE02-6-3 omphacite	S	42.0	−3.15
MVE04-44-6 omphacite	N	84.9	+0.11
MVE04-44-6 omphacite replicate			+0.14
MVE04-44-6 whole rock	N	32.0	−0.06
MVE04-44-6 garnet	N	3.7	−5.23
MVE04-44-7 omphacite	N	86.3	−1.00
MVE04-44-7 whole rock	N	37.0	−0.82
MVE04-44-7 garnet	N	2.7	−4.10
BCG12 whole rock	S	37.0	−4.00
BCG13 whole rock	S	33.0	+0.83
MVE04-14-3 whole rock	S	33.3	+0.75
ACG03-01 omphacite	S	49.5	+1.12
ACG03-01 omphacite replicate	S	50.2	+1.0
ACG03-01 glaucophane	S	36.3	+2.91
ACG03-01 phengite	S	10.3	+0.03
ACG03-01 garnet	S	1.6	+2.7
ACG03-17 omphacite	S	59.0	+0.40
ACG03-17 phengite	S	9.8	−0.94
ACG03-17 garnet	S	3.1	+1.10
Jadeitites and albitites			
MVE03-76-3 jadeite	S	20.0	−1.16
MVE03-76-3 chlorite/magnetite vein	S	12.0	+3.10
MVE03-76-3 pumpellyite	S	2.5	+5.36
MVE02-8-5 jadeitite whole rock	S	34.0	−0.88
MVE04-44-2 jadeitite whole rock	N	84.0	+2.85
JJE01-3-2 jadeite	N	50.0	−1.10
JJE01-3-2 phengite	N	30.0	−0.81
MVJ84-9B jadeite	N	67.0	−1.14
MVJ84-9D jadeite (later vein)	N	51.0	−0.06
MVJ87-14-1 omphacite	N	52.8	+2.39
MVJ84-56-4 albite	N	12.0	−0.79
MVJ84-56-3 albite	N	37.0	−1.50
MVJ84-3-2 phengite	N	12.0	+3.94
MVJ84-29-1 phengite	N	16.0	+1.22
Serpentinite			
MVJ03-84 Cpx	N	0.5	+0.20
Amphibolite			
MVE04-14-4 glaucophane	S	22.0	nd[a]

[a] No data.

Table 2
Lithium concentrations and δ^7Li for mineral separates and whole rock values for Franciscan eclogites, and global jadeitites.

Sample	Li (ppm)	δ^7Li (‰)
Franciscan eclogites (whole rock)		
T90-1b	25.3	+1.30
GL14-2	39.1	−3.90
MH90-1a	25.0	−3.25
T90-5C	31.0	−2.50
Global jadeitites (location and sample name)		
Myanmar MVE2-3-15	36.0	−0.59
Myanmar CJ1	51.0	−0.83
Urals 104278	27.0	+2.46
Japan OKJ00-4-1	28.0	+0.35
Kazakhstan 102029	23.0	+2.24

tions (44 ± 10 ppm 1σ) and lightest δ^7Li (-0.70 ± 0.20‰ 1σ). Jadeitites from the Urals and Kazakhstan have similar Li concentrations (25 ± 3 ppm 1σ) and the heaviest δ^7Li ($+2.35 \pm 0.15$‰ 1σ). The Japanese jadeitite has moderate Li concentrations and isotopes, and is bracketed by the other samples. A calculation of average global jadeitite (including Guatemala) yields a Li concentration $\sim 39 \pm 20$ ppm and $\delta^7\text{Li} = +0.55 \pm 1.70$‰ 1σ, similar to Guatemalan and Franciscan eclogites.

It is interesting to note that these HP–LT rocks have δ^7Li values mostly at or below 0‰, which is uncommon for mafic rocks. The vast majority of MORB, OIB and island arc basalt (IAB) lavas are between δ^7Li of +2‰ and +6‰ (Tomascak et al., 2002, 2008; Elliott et al., 2004; Ryan and Kyle, 2004; Tomascak, 2004; Chan et al., 2006b). Likewise, altered oceanic crust (δ^7Li ~−1 to +20‰) and sediments (δ^7Li ~0 to +12‰) overlap that of mantle and MORB values generally ranging to heavier rather than lighter isotopic values (Chan et al., 1992, 2002c, 2006a; Bouman et al., 2004). HP–LT rocks from Guatemala, the Franciscan and global jadeitites presented here do overlap with δ^7Li from other HP–LT terrains (Zack et al., 2003; Marschall et al., 2007b), suggesting they all underwent similar processing.

4. MODELING

Re-creating the subduction path of HP–LT terrains is challenging because of the many variables involved. Both Guatemalan and Franciscan rocks show evidence for complex metamorphic histories involving fluid metasomatism over a range of depths. Complex fluid histories have also been demonstrated for jadeitites globally (e.g., Sorensen et al., 2006). Below we show that a single stage dehydration model cannot explain the eclogite data. We then develop a simple two-stage approach of (1) prograde dehydration flowed by (2) retrograde hydration/recrystallization or precipitation. We also show that retrograde hydration requires that a small but significant percent of Li be derived from a sediment component. A full discussion of the determination of fractionation factors and partition coefficients used in the modeling can be found in Appendix D.

4.1. Stage 1 – Prograde dehydration of the altered ocean crust

4.1.1. Composition of the AOC

The altered ocean crust (AOC) contains the majority of water in the down-going slab (because it is volumetrically larger than the sedimentary layer), so it is reasonable to assume that it contributes significant Li during dehydration. Estimates of Li concentrations in AOC vary. The uppermost extrusives are probably best represented by the super-composite of site 801 from Kelley et al. (2003), with

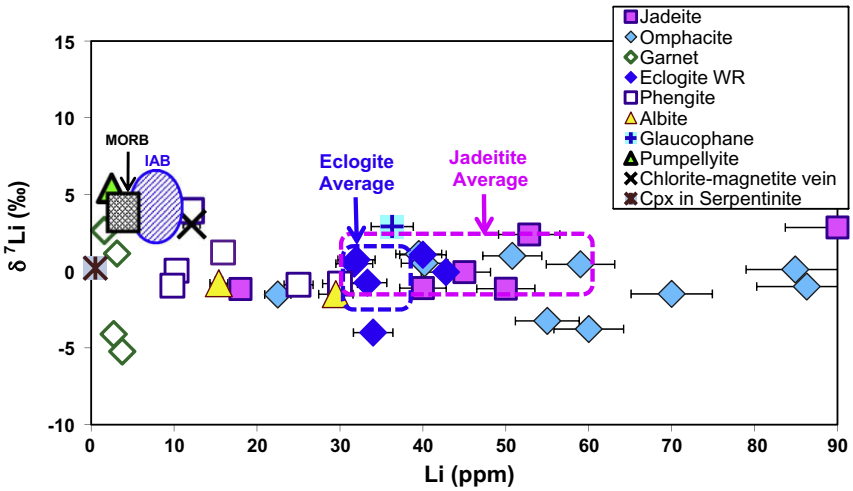

Fig. 4. Li concentration vs. δ^7Li for mineral separates and whole rocks from Guatemala. Mineral separates show relative uniformity of δ^7Li, but Li concentrations vary by a factor of ~50. The average Guatemalan eclogite whole rock is shown in the blue square and average jadeitite in a pink square. Error bars for Li concentration are 7%, and for δ^7Li are the size of the symbol (±0.4‰). MORB, (black hatched box) and island arc basalts (IAB); blue circle with diagonal lines are for reference. (For interpretation of the references to color in this figure legend, the reader is referred to the web version of this article.)

an average Li concentration of ~14 ppm. An estimate for δ^7Li in the upper crust is more difficult, as there are few comprehensive studies of the AOC. Estimates range from ~+4.5‰ from DSDP Hole 595 (Rosner et al., 2005) to ~+10‰ for the upper extrusives from 504B (Chan et al., 2002c). We use an average starting composition of ~+7.5 ± 3‰ as an approximation for the Li isotopic composition of the uppermost crust (Table 3). Estimating δ^7Li for the entire AOC is even more difficult, as there are even fewer measurements of the lower (below extrusive) portions of the ocean crust. Of the few measurements that exist (e.g., ODP holes 504B and 1256), most are drilled into younger Pacific crust (Chan et al., 2002c; Cooper et al., 2004a; Gao et al., 2007). Data from these holes suggest that once below the extrusive portion of the crust (usually the most altered) and into the transition zone and dikes, Li concentrations and δ^7Li generally decrease as water/rock ratios decrease, becoming similar to that of fresh MORB. Thus a weighted average of the upper ~2 km of crust at 504B shows an average Li concentration and δ^7Li very similar to that of fresh MORB (Li ~3.6 ppm and δ^7Li ~3.6‰). If a weighted average were calculated for the whole crust assuming that Li values below the dikes, where water/rock ratios are low, are similar to average MORB, then even a large degree of alteration in the upper extrusives would not significantly move the average of the AOC away from MORB. Therefore, we use the weighted average of hole 504B as an approximate starting composition to represent the bulk crust (Table 3).

Table 3
Starting composition for basalt and sediment components.

	C_o (ppm)	δ^7Li_i (‰)
Basalt source		
Bulk AOC	3.6	+3.6
Upper AOC	14.0	+7.5
Sediment source		
Tonga	15	+7.0
Lesser antilles	65	−0.3
GLiMM	43	+3.0

Starting composition for bulk AOC is an integrated mean of the ocean crust without gabbro from ODP Hole 504B, eastern Pacific (Chan et al., 2002c). The upper AOC Li concentration is from the super-composite of Kelley et al. (2003), with an average δ^7 Li from the uppermost extrusives of holes 504B (Chan et al., 2002c), and DSDP hole 595 (Rosner et al., 2005), western Pacific. Sediment source compositions and GLiMM (global Li mass weighted mean) from Chan et al. (2006a) and Bouman et al. (2004).

4.1.2. AOC dehydration model parameters

The AOC dehydration model was run in nine temperature steps, with partition coefficients and fractionation factors changing at each step (50, 150, 260, 350, 400, 450, 500, 550 and 600 °C). Dehydration estimates are from Schmidt and Poli (2003) and assume that the slab started with ~8 wt% H_2O, losing most of it (~4–6 wt%) over the blueschist facies and blueschist-eclogite transition. Estimated partition coefficients and fractionation factors for Li (Table 4), and the equation for Rayleigh Fractionation, allows for the calculation of Li concentration and δ^7Li remaining in the slab during dehydration, using the following equations:

$$\delta^7Li_{solid} = [(\delta^7Li)_i + 1000]f^{(\alpha-1)} - 1000 \quad (1)$$

$$C_{solid} = C_o(1-F)^{1/D-1} \quad (2)$$

where $(\delta^7Li)_i$ is the initial or starting isotopic composition, α is the fractionation factor, C_o is the initial or starting concentration of Li, D is the bulk partition coefficient, f tracks the fraction of Li lost from the system as a ratio of C_{solid}/C_o, and F is the fraction of liquid relative to the fraction of solid it is in equilibrium with (<1). For example, 1 wt%

Table 4
Model parameters for dehydration of the altered oceanic crust.

H_2O (wt%)	T (°C)	α	$d_{chlorite}$	$d_{smectite}$	$d_{omp/jade}$	d_{cpx}	d_{grt}	d_{pheng}	$D_{integrated}$
0.50	50[a]	1.012	1.7	2.4	–[h]	0.2	–[h]	–	0.35
0.75	150[b]	1.0085	0.80	2.3	–	0.2	–	0.25	0.27
1.00	260[b]	1.0063	0.35	1.9	–	0.2	–	0.25	0.23
1.25	350[c]	1.0050	0.10	1.3	1	0.2	0.008	0.25	0.28
1.50	400[d]	1.0044	0.02	–	1	0.2	0.008	0.25	0.32
0.80	450[e]	1.0039	0.01	–	1	0.2	0.008	0.25	0.36
0.50	500[f]	1.0035	0.005	–	1	0.2	0.008	0.25	0.36
0.36	550[g]	1.0031	0.004	–	1	0.2	0.008	0.25	0.35
0.34	600[g]	1.0028	0.004	–	1	0.2	0.008	0.25	0.35

AOC dehydration path is calculated over multiple temperature intervals. Fractionation factors and percent dehydration change with each temperature step. $D_{integrated}$ is the partition coefficient used for the model, and varies as mineral proportions change with temperature. Individual mineral partition coefficients from Brenan et al. (1998), Berger et al. (1988), including extrapolated data from Berger et al. (1988) for chlorite and smectite, and partition coefficients estimated in this paper. Fractionation factors from Chan et al. (1992, 1993, 2002c), Magenheim et al. (1995), Chan and Kastner (2000) and Wunder et al. (2006).

[a] 91% cpx, 7% chlorite, 2% smectite.
[b] 87% cpx, 7% chlorite, 1% smectite, 5% phengite.
[c] 43% cpx, 3% chlorite, 7% phengite, 17% omphacite, 30% garnet.
[d] 24% cpx, 3% chlorite, 8% phengite, 25% omphacite, 40% garnet.
[e] 19% cpx, 3% chlorite, 8% phengite, 30% omphacite, 45% garnet.
[f] 6% cpx, 3% chlorite, 8% phengite, 33% omphacite, 50% garnet.
[g] 3% cpx, 2% chlorite, 7% phengite, 33% omphacite, 55% garnet.
[h] Not applicable.

H_2O equilibrating with 100% of the solid is $F = 0.01$. Model results are listed in Appendix D.

Fig. 5A shows the initial low-T hydration and calculated solid dehydration paths for the top of the crust and bulk AOC. Dehydration is characterized by a continuous decrease in both δ^7Li and Li concentration. By the time that δ^7Li decreases from its initial bulk crustal value of ~+3.6‰ or upper extrusive value of ~+7.5‰ to Guatemalan- and Franciscan-like values of ~0‰, the Li concentrations left in the crust are ~3 ppm and ~12 ppm, respectively (~14–16% Li loss), which is far less than the average Li concentration in Guatemalan and Franciscan rocks (~30 ppm). This is less of a Li loss than the 50% estimated by Marschall et al. (2007a), but agrees with previous findings that the majority of Li is likely to remain in the crust (Woodland et al., 2002; Savov et al., 2005; Marschall et al., 2007a). These calculated residual solid paths therefore cannot recreate the range of Guatemalan and Franciscan HP–LT data (Fig. 5A).

Trace element compositions of Guatemalan and Franciscan HP–LT rocks suggest that they are not direct representatives of the dehydrated slab, but rather record the influence slab fluids, therefore it is more appropriate to calculate the fluid in equilibrium with the solid paths calculated previously. An instantaneous fluid in equilibrium with the solid crust can be calculated for any step along the solid path using the following equations:

$$\delta^7\mathrm{Li}_{\mathrm{fluid}} = \alpha(1000 + \delta^7\mathrm{Li}_{(\mathrm{solid})}) - 1000 \quad (3)$$

$$\mathrm{Cl} = C_o/D \times (1 - F)^{(1/D-1)} \quad (4)$$

where the symbols are the same as Eqs. (1) and (2).

The starting composition, fractionation factors and partition coefficients remain the same as in the previous calculations. An instantaneous fluid in equilibrium with either the bulk AOC or the topmost part of the crust, at temperatures relevant to these rocks (T ~500 °C), does not have the right combination of high Li concentrations and light isotopic values to reproduce the Guatemalan and Franciscan datasets (Fig. 5B).

4.1.3. Comparison to previous prograde dehydration models

Previous studies (Zack et al., 2003; Bouman, 2004) have modeled Li in the dehydrating ocean crust using simple Rayleigh fractionation models with constant partition coefficients and fractionation factors. Both studies arrived at similar conclusions, with very heavy δ^7Li leaving the slab and metasomatizing the overlying mantle wedge, leaving behind a Li depleted, isotopically light residual slab to be subducted into the deep mantle. More recently Marschall et al. (2007b) modeled the evolution of Li and Li isotopes using the more sophisticated approach of changing T, P, D and α over the course of the calculation, similar to the model presented here. As with previous models, Marschall et al. (2007b) used δ^7Li estimates for average AOC (+10‰) and altered AOC (+11.8‰) that are isotopically heavier than our estimates for bulk crust. Only considering the most altered portions of the AOC will tend to skew results to heavy δ^7Li values for dehydrating fluids. Including the lighter δ^7Li averages measured in the lower volcanics (~+4.6‰), the transition zone (~+1.6‰), and the upper and lower dikes (~+1.8‰) from 504B (Chan et al., 2002c), produces a weighted bulk AOC that has very similar Li systematics to fresh MORB, and is our preferred starting composition. Average δ^7Li starting compositions similar to those from Marschall et al. (2007b) result in fluid compositions at intermediate depths (δ^7Li > +10.5‰) that are heavier than those sampled in arc lavas. They also contrast with lighter δ^7Li values measured in fluid metasoma-

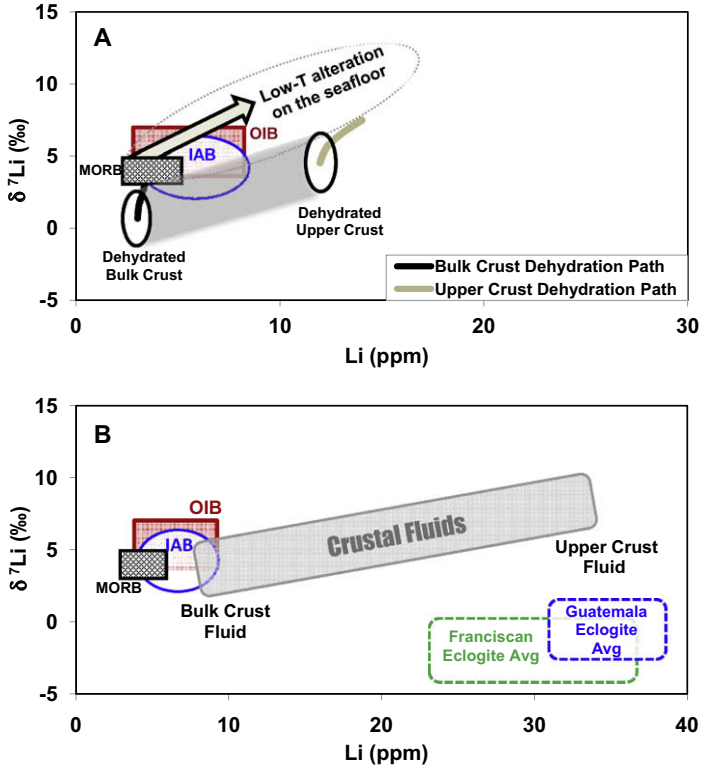

Fig. 5. (A) Results for dehydration of the altered oceanic crust for possible bulk crust and upper crust compositions. Model paths represent the dehydrating (up to 75%) residual solid calculated using the parameters outlined in Table 4. (B) Calculated range in crustal fluids in equilibrium with dehydrated crust at maximum T (500 °C). Blue and green boxes represent average eclogite from Guatemala and the Franciscan respectively. A fluid in equilibrium with only the solid dehydrated crust (grey rectangle) does not have the right combination of high Li concentration and light isotopic ratios to reproduce the average Guatemalan and Franciscan eclogites. MORB, ocean island basalt (OIB) and IAB fields are for reference. (For interpretation of the references to color in this figure legend, the reader is referred to the web version of this article.)

tized samples from Guatemalan and Franciscan HP–LT rocks, global jadeitites presented in this paper (Table 2), and other HP–LT eclogites globally (Zack et al., 2003; Marschall et al., 2007b). Our average calculated fluid composition at comparable temperatures (~+2‰ to +6‰), overlaps with most arc lavas, and can explain the large range in δ^7Li (~15‰) from the recent Agostini et al. (2008) paper with δ^7Li down to -4‰. Therefore, while Marschall et al. (2007b) share some similar modeling assumptions to this paper, results vary due to different starting compositions and partition coefficients.

We have shown that Guatemalan and Franciscan HP–LT rocks cannot represent dehydrated crust, nor can they represent dehydrated crust metasomatized by an AOC fluid alone. Thus another source that is both more Li-rich, and isotopically lighter is needed, which we will show may be sediment.

4.2. Stage 2 – Exhumation and rehydration

Stage two of a simplified model involves exhumation and rehydration of eclogites at or prior to 130 Ma. Exhumation of these HP eclogites and blueschists is thought to have occurred in the shear zone that lies between the down-going plate and hanging wall. Focused fluid flow along this boundary (i.e., in the mélange) likely led to the partial overprinting of the dehydration signal imparted during prograde metamorphism. The enhanced fluid flow within the more permeable mélange also may have facilitated homogenization of the Li isotopic signal (Fig. 4), similar to what has been seen for O–H–N isotopes in other HP environments (Bebout, 1991, 1997; Bebout and Barton, 1993, 2002). This retrograde recrystallization then becomes the dominant geochemical signal in these rocks.

A sedimentary component in the fluid is suggested by the overall trace element patterns, which share similarities to Global Subducting Sediment (GLOSS, Fig. 3), and is supported by Sr and Nd isotope modeling (Simons, 2008). A sediment fluid model can be generated using the same fractionation factors and Rayleigh distillation Eqs. (1)–(4) used for modeling the AOC. Partition coefficients for the sediment model are discussed in Appendix D, and starting compositions are defined below.

4.2.1. Li in sediments

The concentration and δ^7Li of marine sediments span a range of over 70 ppm and ~17‰ (δ^7Li about −2‰ to 15‰) globally (Dean and Parduhn, 1983; Bouman et al., 2004; Chan et al., 2006a). These values reflect sediment type, provenance and diagenetic processes. Clays consistently have the highest Li concentrations (Li ⩽ 80 ppm), as well as isotopically light Li (−1.5‰ to +5‰), making a clay-rich

(e.g., continentally-derived) sediment an excellent candidate for adding light Li to a subduction fluid. Marine volcanics (~14 ppm), and biogenic oozes (≤6 ppm) have lower Li concentrations and generally heavier isotopic values (δ^7Li ~+6‰ to +14.5‰), making these ocean-derived sediments less important for adding high Li concentrations (Chan and Kastner, 2000; Bouman et al., 2004; Chan et al., 2006a).

We have compiled sediment data from the literature in order to determine end-member starting compositions for Li. Included are cores taken from fore-arcs including the Marianas, South Sandwich, Lesser Antilles, Tonga and the Aleutians (Bouman et al., 2004; Chan et al., 2006a). These sediment averages show a negative correlation between Li/Y and δ^7Li (Fig. 6). The end-members of this trend are represented by sediment with a strong continental affinity characterized by high Li/Y and a low δ^7Li (e.g., southern Lesser Antilles), and sediments with little to no continental affinity characterized by lower Li/Y and heavier δ^7Li (e.g., Marianas or Tonga). Calculation of a Global Li Mass-weighted Mean (hereafter GLiMM) in these subduction related sediments has a column integrated concentration of 43 ppm and δ^7Li = 3.01‰ (Chan et al., 2006a). The two sediment end-member representatives (southern Lesser Antilles and Tonga) and GLiMM are used as starting compositions (Table 3) to evaluate the sediments most likely involved in generating the fluid signatures recorded by Guatemalan and Franciscan metabasalts.

4.2.2. Sediment dehydration model

Similar to the AOC dehydration model, the sediment dehydration model consists of multiple steps with increasing T (50, 150, 260, 350, 400, 450, 500, 550 and 600 °C). Fractionation factors remain the same as the AOC model, however, partition coefficients (discussed in Appendix D) vary due to the change in mineralogy. Dehydration estimates for sediments are from Schmidt and Poli (2003) and assume that the sediment initially had ~3.5 wt% H_2O similar to average low grade metapelites from Teng et al. (2007). Water from the dehydrating underlying ocean crust has been added to dehydration estimates of the sediments, as AOC fluid most likely followed a path through the sedimentary layer before metasomatizing rocks in the shear zone or mantle wedge. Model parameters are listed in Table 5, and results are shown in Appendix D. Fluids that are liberated as a result of sediment dehydration (sediment fluids) vary as a function of both composition and T. All model paths have a characteristic initial slight increase in Li concentration and δ^7Li due to the bulk partition coefficient being greater than 1 during the first low-temperature step (T = 50 °C). Bulk partition coefficients change over to incompatible after the first step, and become progressively smaller with increasing temperature (Table 5). Sediments are taken to ~90% dehydration, since some Li is retained in hydrous minerals like phengite, which break down deeper in the system. Sediment derived fluids increase in Li concentration in the order of Tonga < GLiMM < Lesser Antilles.

4.3. Jadeitite as a proxy for fluid composition

If jadeitites directly record the composition of fluid at depth, then global jadeitites (including Guatemala) should provide constraints on the range of fluid compositions involved in metasomatizing HP rocks for environments where jadeitite is precipitated. We have shown that jadeitites from Japan, Kazakstan, the Urals and Myanmar have Li concentrations and δ^7Li similar those from Guatemala, and that similarities in mineralogy and petrography (Sorensen et al., 2006), imply similar processing for these jadeitites (Harlow et al., 2007). A major difference between jadeitite for different locations, however, is that Li concentrations vary by at least a factor of five, suggesting that margins either incorporated different amounts of sediment and/or different compositions of sediment. Using the AOC and sediment fluid results, we have calculated mixing lines between AOC and sediment fluid as a function of T and sed-

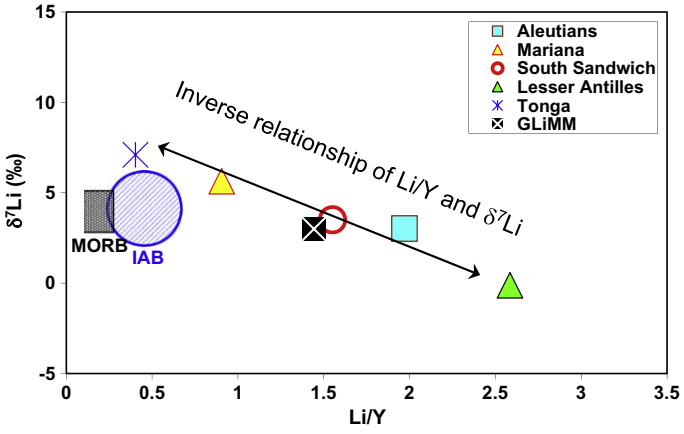

Fig. 6. Li/Y vs. δ^7Li (‰) for averages of marine sediment taken from cores associated with different arcs from around the world (Bouman et al., 2004; Chan et al., 2006a). GLiMM is the Global Li Mass-weighted Mean calculated by Chan et al. (2006a). There is an inverse relationship in the data showing that sediments contributing to the open ocean sediment end-member, represented by Tonga/Mariana, are isotopically heavier and lower in Li concentration than the more continentally influenced sediments derived from South America subducted at the southern Lesser Antilles. This is because the upper continental crust is a reservoir of isotopically light Li (~0‰; Teng et al., 2004).

Table 5
Model parameters for dehydration of sediment.

H_2O (wt%) sediment	H_2O (wt%) sediment + crust	T (°C)	α	$d_{chlorite}$	$d_{smectite}$	$D_{phengite}$	$D_{carbonate}$	$D_{integrated}$
0.30	0.80	50[a]	1.012	1.70	2.40	0.25	0.10	1.13
0.75	1.50	150[b]	1.0085	0.80	2.30	0.25	0.10	0.82
1.25	2.25	260[c]	1.0065	0.35	1.90	0.25	0.10	0.46
1.00	2.25	350[d]	1.0050	0.1	1.30	0.25	0.10	0.22
0.20	1.95	400[e]	1.0043	0.02	–	0.25	0.10	0.15
0.00	0.80	450[e]	1.0038	0.01	–	0.25	0.10	0.14
0.00	0.50	500[e]	1.0034	0.005	–	0.25	0.10	0.14
0.00	0.35	550[e]	1.0031	0.005	–	0.25	0.10	0.14
0.00	0.34	600[e]	1.0028	0.005	–	0.25	0.10	0.14

Model paths are calculated for three different sediment starting compositions (Tonga, southern Lesser Antilles or GLiMM). Dehydration paths are calculated over multiple temperature steps, with a different percent dehydration and fractionation factor at each temperature. $D_{integrated}$ is the partition coefficient used for the model, and varies as mineral proportions, and partition coefficients change with temperature. Individual mineral partition coefficients are estimated in this paper, and from Berger et al. (1988), including extrapolated data from Berger et al. (1988) for chlorite and smectite. Fractionation factors from the same sources as Table 4.

[a] 20% chlorite, 30% smectite, 35% carbonate, 15% phengite.
[b] 20% chlorite, 25% smectite, 35% carbonate, 20% phengite.
[c] 20% chlorite, 15% smectite, 35% carbonate, 30% phengite.
[d] 20% chlorite, 5% smectite, 35% carbonate, 40% phengite.
[e] 20% chlorite, 35% carbonate, 45% phengite.

iment composition (Fig. 7A and B). Fig. 7A shows the results for these mixing lines as a function of T (constant sediment composition). Results suggest that these jadeitites are formed under a limited set of P–T conditions, as most of the jadeitites fall between the 400 and 500 °C mixing lines. In reality, jadeitites sample a variety of fluids during formation (Sorensen et al., 2006), such that their δ^7Li likely records mixtures of fluids (both higher and lower T). Samples lying on the 500 °C mixing line suggest formation at temperatures roughly 100 °C warmer than the maximum temperatures calculated for jadeitite formation (Harlow and Sorensen, 2005; Tsujimori et al., 2006a). This may suggest that either some of the fluids generating the jadeitites originated from deeper in the system, or that jadeitites precipitated from a fluid that was isotopically heavier than the jadeitite solid (i.e., ^{6}Li is preferentially incorporated into the solid phase). In the first scenario, hotter fluids would have likely traveled down pressure and temperature along the shear zone between the hanging wall and down-going slab until they cooled enough to reach saturation, thereby depositing jadeitite. However, this fluid would have to travel down temperature ~100 °C without precipitating out most of its dissolved load along the way. In the second scenario, jadeite and phengite preferentially incorporate ^{6}Li from a fluid phase, such that the jadeitite solid ends up isotopically lighter than the fluid it is in equilibrium with. Wunder et al. (2006) conducted experiments between synthetic spodumene and fluid at 2 GPa and 500–900 °C, and found that ^{7}Li was preferentially partitioned into the fluid at all temperatures. At 500 °C the $\Delta^7Li_{spodumene\text{-}fluid}$ is ~−3.5, suggesting that a Li-rich pyroxene like jadeite in equilibrium with a subduction fluid would be ~3.5‰ lighter than the fluid itself. Extrapolating this experimental relationship to the assumed max T of jadeitite formation (~400 °C) suggests an offset between spodumene and fluid of ~−4.4‰. Wunder et al. (2007) also determined the partitioning of Li isotopes between fluid and mica at the same P, but lower T (300–500 °C) as the previous experiment. Again ^{7}Li is preferentially partitioned into the fluid phase, however, the fractionation was determined to be about half as much as that between spodumene and fluid. Thus, a jadeitite rock precipitating from an aqueous fluid under equilibrium conditions at ~400 °C would be ~3‰ to 3.5‰ lighter than the fluid. Stated another way, the measured jadeitite average of $+0.6 \pm 2.0$‰ for Guatemala would have been in equilibrium with a fluid that was ~+3.5‰ to +4‰, which is comparable to the modeled 400 °C mixing line in Fig. 7A. Plotting a fluid composition in equilibrium with each jadeitite solid (open symbols in Fig. 7A), shows that all could have precipitated at a temperature of ~400 °C or less, which is in line with the temperatures of formation determined by geothermometry and mineral assemblages. Therefore, although deeper fluids could have been incorporated into the jadeitites, it is not required.

Since jadeitites are formed by similar mechanisms over a limited P–T range, then varying the proportions of AOC vs. sediment fluid should reproduce the range of Li concentrations observed. Fig. 7B shows the results of the AOC-sediment fluid mixtures as a function of composition ($T = 400$–500 °C). Jadeitites from Myanmar suggest the greatest sediment fluid influence with up to 20% of the Li contributed by a sediment. Jadeitites from Kazakhstan, the Urals and Japan have a smaller apparent sediment fluid influence of roughly 5–7%, while Guatemalan jadeitites are between these other localities with sediment fluid proportions of ~10%. An apparent ~5% sediment fluid contribution for Japan is consistent with estimates of Moriguti and Nakamura (1998a) who used Li and Pb isotopes to determine a ~3% sediment contribution for Japanese arc lavas. These mixing proportions are also supported by mixing models of Sr and Nd isotopes, which point to a well-mixed fluid for the metasomatism of fresh eclogite, and blueschist mineral separates from Guatemala and the Franciscan (Simons,

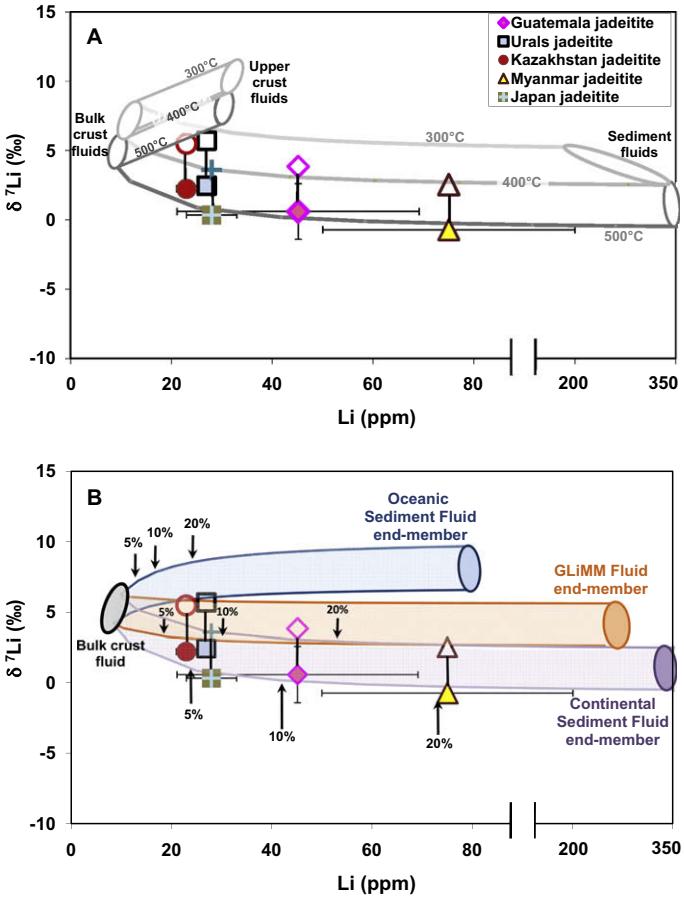

Fig. 7. Subduction fluid mixing model showing. (A) Binary mixtures of a sediment fluid end-member and bulk AOC fluid as a function of T for a single sediment fluid composition (Lesser Antilles). Fluids generated by the uppermost crust alone are shown for comparison. The mixing model shows that jadeitite solids can be represented by a narrow range of temperatures which are generally greater than those estimated for jadeitite formation (~400 °C). However, the fluids that precipitated these solids (shown as attached open symbols) are in agreement with max T estimates. (B) Li mixing model results for jadeitites showing binary mixtures between sediment fluid and bulk AOC fluid end-members, where mixing fields are a function of changing sediment composition at constant T. The continental sediment field represents the Lesser Antilles end-member, while the oceanic sediment field represents the Tonga sediment end-member. Arrows show where mixtures are made up of 20%, 10% and 5% sediment fluid. Jadeites show that subduction fluids are dominated by the AOC. Note change in scale on x-axis.

2008). The jadeitite mixing model (Fig. 7B) also suggests that the sediment fluid compositions that best fit the global jadeitite data are ones with characteristics similar to continental sediments (e.g., southern Lesser Antilles) and perhaps GLOSS (GLiMM). This is especially true for jadeitites from Guatemala and Myanmar, while the Urals, Kazakhstan and possibly Japan could be modeled with sediment similar to GLOSS. Additional data is needed to confirm this.

4.4. Multi-stage model for the origin of HP–LT oceanic eclogites

Using the insight that jadeitites provide on AOC vs. sediment fluid proportions, and AOC and sediment modeling results, allows us to model the formation of the Guatemalan and Franciscan eclogites in a two-stage process. Fig. 8A shows mixing paths between a dehydrated eclogite (bulk crust) at max T (500 °C), and subduction fluids that vary as a function of T (500–600 °C), sediment composition (Tonga, GLiMM and Lesser Antilles) and AOC-sediment proportion (~5% to 15% sediment). Mixtures are dominated by the fluid end-member because of the higher concentrations of Li in the fluid. Of the three hybrid AOC-sediment fluid compositions investigated (Fig. 8A), Guatemalan and Franciscan eclogites are best modeled as dehydrated bulk eclogite overprinted by fluids derived from an AOC-continental-like (Lesser Antilles) sediment, in which 5–10% of the Li is derived from the sediment fluid component.

The addition of a field representing the upper ocean crust (Fig. 8B) extends the range of possible dehydrated eclogite compositions at 500 °C (all other parameters from Fig. 8A remain the same). Adding other eclogites of oceanic origin, like Syros and Tianshan HP–LT eclogites (Marschall et al., 2007b) shows that they can be modeled as dehydrated eclogite plus or minus small amounts of subduction fluid, most likely added during exhumation. This result is supported by field evidence from Syros, where meta-igneous blocks are enclosed in mafic–ultramafic schists, and

have been interpreted as blocks or fragments of oceanic crust, mechanically separated from the slab, and entrained into a subduction channel or shear zone with buoyant serpentinite and other exhuming material (Shreve and Cloos, 1986; Engi et al., 2001; Gerya et al., 2002; Marschall et al., 2006). Three of the four eclogite localities in Fig. 8B can be modeled as mixtures between dehydrated AOC and an AOC-continental-type fluid at 500–600 °C. Samples from Syros are both eclogite and meta-plagiogranite (Marschall et al., 2007b), and have a wide range of Li concentrations and isotopic values, making it difficult to identify a specific sediment type without further details. Similar to jadeitite model results, Franciscan and Guatemalan eclogites show temperatures that are up to 100 °C higher than estimates of max T from thermometry. Assuming the partitioning behavior of Li into omphacite is similar to that of jadeite (Appendix D), then calculating a δ^7Li for the metasomatic fluid in equilibrium with omphacite produces a new set of data points that are shifted to heavier δ^7Li (Fig. 8C). Fluid values are calculated using the results of Wunder et al. (2006, 2007) and assumes roughly half the eclogite is composed of pyroxene + phengite for samples where petrography is not available. This correction produces a shift in δ^7Li of ~+1.5‰, which places the equilibrium Guatemalan eclogite fluid within the field generated by mixtures with an AOC-continental sediment fluid at 400–500 °C, consistent with Guatemalan eclogite max T estimates. Max T estimates for some Franciscan eclogites are slightly higher, which is perhaps why most have lighter δ^7Li values. Thus, by using the estimated δ^7Li of the fluid composition in equilibrium with the eclogites, rather than the eclogite WR solids, we can alleviate the misfit between the model results and the samples themselves. If this proposed mechanism is correct, then deeper fluids (i.e., those hotter than ~500 °C) may not be involved in the metasomatism of these HP–LT eclogites during exhumation. However, a more detailed investigation of how individual minerals may fractionate Li isotopes as a function of T is needed in order to fully evaluate this mechanism.

The mixing models presented here demonstrate the importance of including sediments when modeling Li in a subduction fluid, as sediment has the potential to provide greater amounts of Li, and lighter isotopic starting values than the AOC alone. HP–LT rocks can be explained by overprinting of dehydrated eclogite with fluids that vary as a function of T, sediment composition and AOC-sediment proportion. Sediment and AOC are assumed to be the major Li reservoirs in the slab, as calculated budgets for the serpentinized lithospheric mantle appear to be of less significance (Vils et al., 2008).

4.5. Non-equilibrium fraction of Li

Kinetic fractionation of Li isotopes has been called upon recently as a possible mechanism for some HP–LT rocks that seemingly cannot be explained by models using simple Rayleigh distillation (e.g., Marschall et al., 2007b; Marschall and Pogge von Strandmann, 2008). However, non-equilibrium processes, often resulting from diffusion, have most often been invoked to explain the Li isotopic disequilibrium found inter- and intra-mineral in mantle xenoliths metasomatized by mantle melts (e.g., Ludstrom et al., 2005; Tang et al., 2007; Rudnick and Ionov, 2007; Jeffcoate et al., 2007; etc.). Marschall et al. (2007b) invoked a diffu-

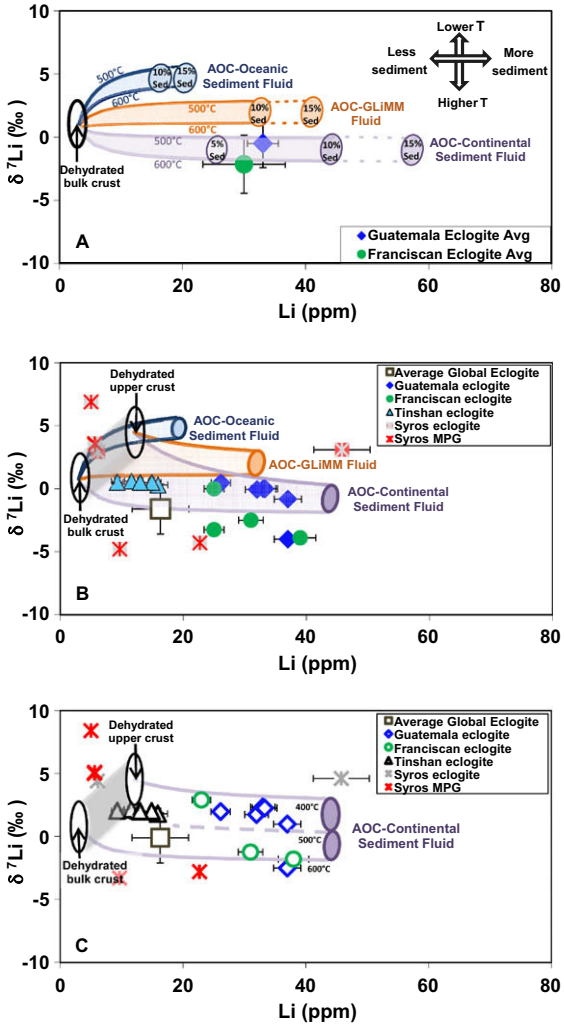

Fig. 8. Li model results for HP–LT whole rock eclogites. (A) Fields are binary mixtures between a dehydrated eclogite solid (bulk crust) at 500 °C, and fluid end-members that vary as a function of sediment-AOC proportion (5–15% sediment), T (500–600 °C), and composition. Sediment compositions are represented by an oceanic sediment end-member (Tonga), a continental-type sediment end-member (Lesser Antilles) and the global average GLiMM. (B) Mixing model for eclogites (same as A), with fixed proportion of sediment fluid (10%). A field is added for the upper AOC, showing a range of possible compositions for dehydrated residual eclogite. Individual data points are whole rock eclogites from around the world thought to have oceanic crust as a protolith, and comparable facies conditions. Syros, Tianshan and average global eclogite from Marschall et al. (2007b). (C) Model results for fluids calculated to be in equilibrium with whole rock eclogites in (B), based on their proportions of phengite and pyroxene. Fluid fields are calculated with a fixed sediment composition (continental-type) and proportion (10%) for $T = 400$, 500 and 600 °C. Calculated δ^7Li of fluids is in good agreement with thermobarometric estimates (below 600 °C) for these rocks.

sion related fractionation to explain high Li concentrations and very light δ^7Li for HP–LT eclogites in their study. However, extreme values (e.g., ~−22‰) were the exception, with the majority (~80%) of their eclogites falling within the same total range of δ^7Li defined by Guatemalan samples (~+5‰ to −5‰). Additionally, mineral separates in Guatemalan rocks do not show the same large inter-mineral offsets in δ^7Li as those often displayed in mantle xenoliths (Fig. 4). For example, coexisting minerals with different mineral structures, like jadeite and phengite in jadeitite, and omphacite and phengite in eclogite show small, but consistent offsets in δ^7Li (~0.5‰ to 1‰). Mineral separates and whole rocks occupy a small total range in δ^7Li (-0.1 ± 4.5‰ 2σ) compared to those in suites where a non-equilibrium mechanism has been invoked (e.g., ~<40‰, Jeffcoate et al., 2007). Garnet separates in Guatemala are the only exception, as garnet is offset to slightly heavier δ^7Li than omphacite in sample TT03-01 and lighter δ^7Li in MVE04-44-6 and MVE04-44-7 (Table 1). It is important to note, however, that MVE04-44-6 and MVE04-44-7 are northern eclogites which underwent a second metamorphic event, and are anomalous in their trace element patterns and radiogenic isotopes. Additionally, low concentrations of Li in garnet can be more easily perturbed by later geologic events than the higher Li concentration omphacites/jadeites. Thus it is not likely that diffusion has played a dominant role in modifying Guatemalan Li concentrations and isotopic compositions for HP–LT rocks. It is more difficult to assess the role of Li diffusion in Franciscan rocks, as only whole rock powders were digested, however, the range of δ^7Li in Franciscan eclogites is comparable to not only Guatemalan eclogite whole rock values, but to the majority (~80%) of HP–LT eclogites measured (e.g., Zack et al., 2003; Marschall et al., 2007b). Diffusion in general may be less important as a mechanism in subduction related rocks recrystallized under higher water/rock ratios, such as those metasomatized in a shear zone. Thus localized, extreme δ^7Li fractionations found in some HP–LT rocks are likely to be the result of a non-equilibrium process, suggesting that while kinetic fractionation of Li isotopes may occur in a subduction setting, it is probably not the major first order process controlling δ^7Li in eclogites.

5. DISCUSSION

5.1. What do exhumed eclogites represent?

Although exhumed HP–LT rocks may provide information about prograde and retrograde subduction conditions, δ^7Li recorded by HP–LT eclogites with strong retrograde fluid overprints (e.g., Guatemala), may not be representative of all subduction zone fluids. This is because HP–LT eclogites are rocks that were subducted and exhumed, and therefore likely record the conditions in the subduction zone just prior to, or during a collision. If these collisions involved at least one continental block or mature arc, then isotopically light continental material (~0‰; Teng et al., 2004) could be introduced at the margin via sediment or possibly by subduction erosion, skewing the δ^7Li of subduction fluids to lighter isotopic values. Guatemalan and Franciscan eclogites presented here, as well as other HP–LT eclogites, like those from Trescolmen with very radiogenic ^{87}Sr/^{86}Sr and enclosed in mica schist (Becker et al., 1999; Zack et al., 2003), are possible examples of this phenomenon. Thus these eclogites may have recorded an end-member subduction fluid, best represented by an AOC-continental-type fluid (Fig. 8). Given the AOC-sediment proportions (~90:10) discussed previously, and T ~300–600 °C, an AOC-continental sediment fluid would generate a range in δ^7Li ~−1.5‰ to +7.5‰, (Appendix D). Calc-alkaline lavas from Anatolia (Agostini et al., 2008) show a similar range in δ^7Li (−4 to +8‰), consistent with the subduction of continental material. The geographic nature of Anatolia (surrounded by Africa and Europe), as well as elevated ^{87}Sr/^{86}Sr ratios (0.707–0.709) in the same lavas, support this argument. Thus margins that incorporate continental materials are likely to have δ^7Li that range to lighter isotopic values, representing an end-member in the spectrum of Li isotopic compositions. Therefore, the best δ^7Li approximation for average subduction fluid may be a mix of AOC and GLiMM (Appendix D).

5.2. Implications for the composition of the mantle wedge and arc lavas

Arc volcanics have long been recognized to have trace element patterns characteristic of chemical and mass transfer from the down-going slab to the overlying mantle wedge over a range of depths. It has been speculated that since Li is both fluid mobile and a light stable isotope, that δ^7Li in arc lavas should be highly variable, reflecting the changing fractionation of Li over a range of T, the regional sediments, and variably altered ocean crust. However, measurements of Li isotopes in arc lavas globally have not been as isotopically heavy, nor as variable as expected, with most overlapping the range of MORB (Fig. 5). The fairly consistent range of δ^7Li for arcs world-wide (~+2‰ to +6‰), suggest that Li is being controlled by a common process or component.

Tomascak et al. (2002) addressed the limited range of δ^7Li in arc lavas by proposing a mechanism that preferentially affected Li more than other trace elements in the slab fluid. The mechanism, similar to the chromatographic column effect (e.g., Navon and Stolper, 1987), involves the exchange of heavy, slab-derived Li with Li from the depleted mantle wedge (e.g., olivine), thereby obscuring the slab contribution. The exchange of Li was proposed because Li is only moderately incompatible in many mantle phases and thus easier to exchange than more highly incompatible elements like B (Ryan and Langmuir, 1987). We present two alternatives to this model to explain the fairly constant δ^7Li composition in arc magmas. The first is a mechanism whereby Li in slab fluids does not effectively reach the arc source region because it is efficiently trapped by metasomatic minerals in veins (e.g., jadeitite), and the second is that there is a component common to all subduction zone fluids which buffers the range of Li isotopes metasomatizing the wedge.

We estimate that only a fraction (~15–30%) of the initial Li subducted leaves the slab during shallow and intermedi-

ate subduction, because Li is moderately incompatible to roughly compatible in many metamorphic and metasomatic minerals commonly formed during subduction (e.g., omphacite, jadeite, phengite, amphibole, etc.). This means that although slab fluids (including sediments) are likely to have initially high concentrations of Li, once they enter the chemical disequilibrium of the mantle, processes like serpentinization are likely to promote the precipitation of veins with metasomatic minerals that may accommodate Li. Thus Li may be efficiently trapped in veins before it reaches the arc source region, thereby diluting the slab Li contribution, and having the depleted mantle ($\sim+3.5 \pm 0.5‰$; Jeffcoate et al., 2007) dominate the Li isotope signal in arc lavas.

The second alternative relies on a common component to buffer the range of Li isotopes observed in arcs. Jadeitites from five different locations presented in this paper point to AOC fluids as the dominant source (~90–95%) of Li in subduction fluids at the moderate to shallow depths where jadeitite is generated. This is consistent with proportions estimated previously using Li and other geochemical tracers (e.g., Moriguti and Nakamura, 1998a; etc.), and suggests that the Li budget of the AOC is what buffers δ^7Li at arcs world-wide. If this is the case, the implication is that the Li budget for most of the ocean crust, when averaged over the whole crust, is relatively similar, and that age or degree of alteration in the uppermost crust is less important. Therefore, even if a wide range of δ^7Li in sediments (e.g., $-0.3‰$ for S. Lesser Antilles, $+3‰$ for GLiMM and $+7‰$ for Tonga) is subducted at margins, the dominance of AOC fluids for Li, especially at greater depths, buffers the total range of Li isotopes, such that subduction fluids at moderate depths average out to be similar to that of the depleted mantle (Appendix D). This could explain why δ^7Li values in arc lavas largely overlap with those of MORB (i.e., mantle) values. Thus, with an AOC buffer, no large scale exchange of slab Li for mantle Li is needed since the Li isotopic character of the slab fluid is already similar to that of the mantle wedge. Although we cannot eliminate any of these mechanisms for generating fairly consistent δ^7Li in arc lavas, we prefer the AOC fluid buffer mechanism. However, given the complexity of the system, it may be a combination of all of the above mechanisms that operate at subduction zones.

5.2.1. Evolution of δ^7Li with dehydration

Our modeling, similar to previous results, suggests that δ^7Li in subduction fluids becomes isotopically lighter as dehydration proceeds with depth. At shallow depths (i.e., $T \leqslant 300$ °C), fluids are isotopically heavier ($\sim+12 \pm 3‰$) than depleted mantle wedge peridotite, which results in a shift to isotopically heavier values for the shallow wedge. These heavy δ^7Li values have been recorded in shallow pore fluids from Costa Rica (Chan and Kastner, 2000) and serpentinite mud volcanoes in the Mariana forearc (Benton et al., 2004), and likely reflect a variety of processes including low-T diagenesis, squeezing out shallow pore fluids, or mixtures of these with isotopically heavier seawater. At moderate depths (temperatures in the slab of $\sim \geqslant 300$ °C), our modeling suggests that metasomatism of the wedge is predominantly done by fluids with δ^7Li that overlap values of the depleted mantle ($+4 \pm 3‰$), regardless of sediment type (Appendix D). This result differs from previous models which continue to have isotopically heavy values (i.e., $\geqslant+10‰$) metasomatizing the wedge at moderate depths and deeper. Our results are supported by the range of δ^7Li recorded in Guatemalan and Franciscan HP–LT rocks, and the fluids calculated to be in equilibrium with these rocks (-2 to $+4‰$; Figs. 7 and 8C). Guatemalan and Franciscan values may provide the lower limits to the range of δ^7Li in subduction fluids, as these rocks have been modeled as having an end-member sediment contribution from a continental-type sediment. We therefore propose that the heaviest isotopes ($\geqslant+10‰$) primarily metasomatize the forearc and shallow corner of the wedge, and as dehydration proceeds at deeper levels both slab and fluids evolve to lighter values. Thus, metasomatism of the mantle wedge at moderate depths ($T > 300$ °C) is done predominantly by fluids with δ^7Li that overlap values of the depleted mantle and arc lavas world-wide ($\sim+1‰$ to $+7‰$).

5.3. Implications for the composition of the dehydrated slab and recycled component

Model results indicate approximately 3 ppm Li is left in the bulk crust at $T = 500$ °C (~12 ppm for the top of the slab), which is similar to what has been predicted by the Marschall et al. (2007b) model (~4 ppm). This represents a loss of only ~15% of the original Li, suggesting that the majority of Li could be conserved within the slab and subducted past subarc depths. Support for deep subduction of Li comes from studies of Li in diamond inclusions, which found that lower mantle phases like ferropericlase and majoritic garnet are sinks for Li with increasing pressure (Seitz et al., 2003). This suggests that some Li that makes it past the subduction factory could remain in the deeper mantle. However, further dehydration of the slab above 500 °C could lower Li concentrations to those estimated for the depleted mantle (~1–1.5 ppm; Ryan and Langmuir, 1987; Eggins et al., 1998; Seitz and Woodland, 2000). Therefore, based on our model for AOC dehydration, the concentration of Li in the recycled bulk ocean crust (~1–3 ppm) should not be a key characteristic in indentifying this source in the mantle. The more identifiable characteristic may be the isotopic composition of the recycled bulk crust ($\delta^7\text{Li} \leqslant +1 \pm 3‰$) or perhaps upper crust ($\sim+5 \pm 3‰$), which could be isotopically distinct from the depleted mantle and may therefore result in mantle Li isotopic heterogeneity.

Overlapping averages in δ^7Li between arc lavas ($+4.2 \pm 1.4‰$ 1σ) and OIB ($+4.9 \pm 0.9‰$ 1σ) (Moriguti and Nakamura, 1998a; Tomascak et al., 1999b, 2000; Chan et al., 2001, 2002a,b, 2006b; Chan and Frey, 2003; Bouman, 2004; Leeman et al., 2004; Ryan and Kyle, 2004; Nishio et al., 2005) have been used to suggest a common source; the metasomatized subarc mantle. Fig. 5 illustrates the overlap in OIB, IAB and to some extent MORB source regions. However, it is possible that this is not a unique solution. For example, quantitative trace element modeling from Donnelly et al. (2004) and Cooper et al. (2004b) sug-

gest generating the recycled component from a low-degree melt of the dehydrated slab below the depths of subduction processing (e.g., >150 km). It is difficult to know if such a melt would reflect the bulk or upper crust δ^7Li values calculated here, and therefore it is difficult to evaluate this potential mechanism at this time. Additionally, there is relatively little comprehensive Li data for ocean island lavas at present, so it is difficult to fully resolve the OIB component in Li isotope space alone. Additional Li isotope data is needed, and it should be compared with other geochemical parameters to address crustal recycling.

6. CONCLUSIONS

- HP–LT rocks in serpentinite mélange from Guatemala and the Franciscan complex in California represent blocks of a down-going slab and pieces of the base of the mantle wedge at two subduction zones. Eclogites record both prograde and retrograde (dominant) subduction paths. Low retrograde temperatures and multiple generations of hydrous phases suggest metasomatism by an aqueous fluid. Jadeitites are interpreted as direct precipitates from this fluid (formed in the overlying mantle wedge), and as such best represent the fluid end-member.
- Trace element patterns for Guatemalan and Franciscan rocks resemble arc volcanics, with large enrichments in fluid mobile elements (Cs, Rb, Ba, K, Pb, Li). Enrichments in Th and Ba, as well as the high concentrations of Li in mineral separates and whole rocks ($\leqslant$90 ppm) suggest the involvement of sediment. Previous work on the Franciscan has suggested a MORB protolith, which is supported by the MORB-like HREE and HFSE concentrations for Guatemalan and Franciscan eclogites presented here.
- Global jadeitites can be modeled as simple mixtures of AOC fluid ($\sim$90–95%) and sediment fluid ($\sim$5–10%). Subduction fluid compositions vary as a function of T, sediment type, and proportion of sediment fluid to AOC fluid, however the AOC fluid appears to be the dominant component.
- Guatemalan and Franciscan eclogites can be modeled using a two-stage process involving (1) AOC dehydration during prograde metamorphism and (2) rehydration of eclogite blocks by a subduction fluid, primarily during collision and exhumation. The small total range in δ^7Li along with small inter-mineral δ^7Li differences suggest that greater fluid flow in the shear zone between the plates may help homogenize the δ^7Li signal, and that kinetic fractionation is less important in this setting. Metasomatism of dehydrated eclogite blocks at intermediate depths reproduces Guatemalan and Franciscan eclogite data, as well as other HP–LT terrains of oceanic origin (e.g., Tianshan, China and Syros, Greece).
- Modeling the dehydration ($\sim$75%) of the bulk AOC results in a mantle reservoir that is isotopically light ($\sim\leqslant+1 \pm 3‰$) compared to the depleted mantle, and relatively low in Li concentration ($\sim\leqslant$3 ppm). The most altered part of the crust (uppermost extrusives), may retain higher Li concentrations ($\sim$12 ppm) than the bulk crust, and an isotopically heavier signature ($\sim+5 \pm 3‰$). The complementary reservoir to the bulk crust is the metasomatized mantle wedge. A subduction fluid with an AOC–GLOSS composition over the full range of model temperatures (50–600 °C) gives an average δ^7Li fluid composition ($\sim+7 \pm 5‰$ 1σ) that is isotopically heavier than the depleted mantle. If the lowest temperature steps are excluded (50–260 °C) as too cold to participate in circulation of the mantle wedge, then the average fluid ($\delta^7\text{Li} = +4 \pm 2.3‰$ 1σ, is indistinguishable from depleted mantle. Given the overlap between OIB, IAB and MORB in δ^7Li space, it is difficult to fully resolve these components with the current data available. Additional Li isotope data is needed, and should be compared with other geochemical parameters to distinguish between potential recycled sources.

ACKNOWLEDGMENTS

We would like to thank Jinny Sisson, Tatsuki Tsujimori, Sidney Hemming and Jackie Dixon for their insight and editing. We would also like to thank A.E. Ryerson, Horst Marschall, Paul Tomascak, Thomas Zack, Samuel Agostini, Jeff Ryan and an anonymous reviewer for their help and useful comments. Funding for this work was made available by the National Science Foundation (EAR 0309832, EAR 039320 and EAR 0309116).

APPENDIX A. SUPPLEMENTARY DATA

The Supplementary data contains detailed mineralogy and petrology sample information (Appendix A), a full Li methods section (Appendix B), trace element compositions (Appendix C) and modeling results as well as a discussion of partition coefficients and fractionation factors used in the modeling (Appendix D). Supplementary data associated with this article can be found, in the online version, at doi:10.1016/j.gca.2010.02.033.

REFERENCES

Agostini S., Ryan J. G., Tonarini S. and Innocenti F. (2008) Drying and dying of a subducted slab: coupled Li and B isotope variations in Western Anatolia Cenozoic Volcanism. *Earth Planet. Sci. Lett.* **272**, 139–147.

Altherr R., Topuz G., Marschall H., Zack T. and Ludwig T. (2004) Evolution of a tourmaline-bearing lawsonite eclogite from the Elekdag area (Central Pontides, N Turkey): evidence for infiltration of slab-derived B-rich fluids during exhumation. *Contrib. Mineral. Petrol.* **148**, 409–425.

Bebout G. E. (1991) Field-based evidence for devolatilization in subduction zones: implications for arc magmatism. *Science* **251**, 413–416.

Bebout G. E. (1997) Nitrogen isotopes tracers of high-temperature fluid–rock interactions: case study of the Catalina Schist, California. *Earth Planet. Sci. Lett.* **151**, 77–91.

Bebout G. E. and Barton M. D. (1993) Metasomatism during subduction: products and possible paths in the Catalina Schist, California. *Chem. Geol.* **108**, 61–92.

Bebout G. E. and Barton M. D. (2002) Tectonic and metasomatic mixing in a high-T, subduction-zone mélange – insights into the geochemical evolution of the slab-mantle interface. *Chem. Geol.* **187**, 79–106.

Bebout G. E., Bebout A. E. and Graham C. M. (2007) Cycling of B, Li, and LILE (K, Cs, Rb, Ba, Sr) into subduction zones: SIMS evidence from micas in high-P/T metasedimentary rocks. *Chem. Geol.* **239**, 284–304.

Beck P., Chaussidon M., Barrat J. A., Gillet P. and Bohn M. (2006) Diffusion induced Li isotopic fractionation during the cooling of magmatic rocks: the case of pyroxene phenocrysts from nakhlite meteorites. *Geochim. Cosmochim. Acta* **70**, 4813–4825.

Becker H., Jochum K. P. and Carlson R. W. (1999) Constraints from high-pressure veins in eclogites on the composition of hydrous fluids in subduction zones. *Chem. Geol.* **160**, 291–308.

Benton L. D. and Tera F. (2000) Lithium isotope systematics of the Marianas revisited. *J. Conf. Abstr.* **5**, 210.

Benton L. D., Ryan J. G. and Savov I. P. (2004) Lithium abundance and isotope systematics of forearc serpentinites, Conical Seamount, Mariana forearc: insights into the mechanics of slab-mantle exchange during Subduction. *Geochem. Geophys. Geosyst.* **5**, 2004GC000708.

Berger G., Schott J. and Guy C. (1988) Behavior of Li, Rb, and Cs during basalt glass and olivine dissolution and chlorite, smectite and zeolite precipitation from seawater: experimental investigations and modelization between 50° and 300 °C. *Chem. Geol.* **71**, 297–312.

Bouman C. (2004) Lithium isotope systematics at subduction zones. Ph. D. thesis, University of Amsterdam.

Bouman C., Elliot T. and Vroon P. Z. (2004) Lithium inputs to subduction zones. *Chem. Geol.* **212**, 59–79.

Brenan J. M., Ryerson F. J. and Shaw H. F. (1998) The role of aqueous fluids in the slab-to-mantle transfer of boron, beryllium, and lithium during subduction: experiments and models. *Geochim. Cosmochim. Acta* **62**, 3337–3347.

Brooker R. A., James R. H. and Blundy J. D. (2004) Trace elements and Li isotope systematics in Zabargad peridotites: evidence of ancient subduction processes in the Red Sea mantle. *Chem. Geol.* **212**, 179–204.

Brueckner H. K., Gilotti J. and Nutman A. P. (1998) Caledonian eclogite-facies metamorphism of early Proterozoic protoliths from the North-East Greenland Eclogite Province. *Contrib. Mineral. Petrol.* **130**, 103–120.

Brueckner H. K., Hemming S., Sorensen S. and Harlow G. E. (2005) Synchronous Sm–Nd mineral ages from HP terranes on both sides of the Motagua Fault of Guatemala: convergent suture and strike slip fault? *Eos Trans. AGU, 86(52), Fall Meet. Suppl, Abstr.*, T23D-04.

Brueckner H. K., Simons K. K., Sorensen S. S., Harlow G. E. and Hemming S. R. (2007) Metasomatism of mantle-derived mafic and ultramafic rocks: Seawater? Subducted Slab? Sediment? Mantle wedge? or Continental crust? *Eos Trans. AGU 88(23), Joint Assembly Suppl., Abstr.*, H33E-02.

Brueckner H. K., Avé Lallemant H. G., Sisson V. B., Harlow G. E., Hemming S. R., Martens U., Tsujimori T. and Sorensen S. S. (2009) Metamorphic reworking of a high pressure–low temperature mélange along the Motagua fault, Guatemala: a record of Neocomian and Maastrichtian transpressional tectonics. *Earth Planet. Sci. Lett.* **284**, 228–235.

Bryant C. J., McCulloch M. T. and Bennett V. C. (2003) Impact of matrix effects on the accurate measurement of Li isotope ratios by inductively coupled plasma mass spectrometry (MC-ICPMS) under "cold" plasma conditions. *J. Anal. At. Spectrom.* **18**, 734–737.

Chan L.-H. and Edmond J. M. (1988) Variation of lithium isotope composition in the marine environment: a preliminary report. *Geochim. Cosmochim. Acta* **52**, 1711–1717.

Chan L.-H. and Frey F. A. (2003) Lithium isotope geochemistry of the Hawaiian plume: results from the Hawaii Scientific Drilling Project and Koolau Volcano. *Geochem. Geophys. Geosyst.* **4**, 2002GC000365.

Chan L.-H. and Kastner M. (2000) Lithium isotopic compositions of pore fluids and sediments in the Costa Rica subduction zone: implications for fluid processes and sediment contribution to the arc volcanoes. *Earth Planet. Sci. Lett.* **183**, 275–290.

Chan L.-H., Edmond J. M., Thompson G. and Gillis K. (1992) Lithium isotopic of submarine basalts: implications for the lithium cycle in the oceans. *Earth Planet. Sci. Lett.* **108**, 151–160.

Chan L.-H., Edmond J. M. and Thompson G. (1993) A lithium isotope study of hot springs and metabasalts from mid-ocean ridge hydrothermal systems. *J. Geophys. Res.* **98**, 9653–9659.

Chan L.-H., Gieskes J. M., You C. F. and Edmond J. M. (1994) Lithium isotope geochemistry of sediments and hydrothermal fluids of the Guaymas Basin, Gulf of California. *Geochim. Cosmochim. Acta* **58**, 4443–4454.

Chan L. -H., Leeman W. P. and Tornari S. (2001) Lithium isotope compositions of South Sandwich Arc and Southwest Washington Cascades: a comparative study of arc processes. *Eos Trans. AGU, 82(47), Fall Meet. Suppl., Abstr.*, V12E-09.

Chan L.-H., Leeman W. P. and You C.-F. (2002a) Lithium isotopic composition of Central American volcanic arc lavas: implications for modification of subarc mantle by slab-derived fluids: correction. *Chem. Geol.* **182**, 293–300.

Chan L. -H., Leeman W. P., Tornari S. and Singer B. (2002b) Lithium and boron isotopes in the Aleutian Islands: contributions of marine sediments to island arc magmas. *Eos Trans. AGU, 83(47), Fall Meet. Suppl., Abstr.*, V61D-11.

Chan L.-H., Alt J. C. and Teagle D. (2002c) Lithium and lithium isotope profiles through the upper oceanic crust: a study of seawater-basalt exchange at ODP Sites 504B and 896A. *Earth Planet. Sci. Lett.* **201**, 187–201.

Chan L.-H., Leeman W. P. and Plank T. (2006a) Lithium isotopic composition of marine sediments. *Geochem. Geophys. Geosyst.* **7**, 2005GC001202.

Chan L., Hart S. R., Blusztajn J. S., Lassiter J. C., Frey F. A. and Hauri E. H. (2006b) Lithium isotopic composition of mantle plumes and the distribution of lithium isotopes among Earth's reservoirs. E*os Trans. AGU, 87(52), Fall Meet. Suppl., Abstr.*, V34B-07.

Chan L.-H., Lassiter J., Hauri E. H., Hart S. R. and Blusztajn J. (2009) Lithium isotope systematics of lavas from the Cook–Austral Islands: constraints on the origin of HIMU mantle. *Earth Planet. Sci. Lett.* **277**, 433–442.

Cooper K. M., Elliott T. R. and Teagle D. A. H. (2004a) Lithium isotopic composition of altered oceanic crust at ODP Site 1256, Leg 206. *Geochim. Cosmochim. Acta* **68**(Suppl. 1), A44.

Cooper K. M., Eiler J. M., Asimow P. D. and Langmuir C. H. (2004b) Oxygen isotope evidence for the origin of enriched mantle beneath the mid-Atlantic ridge. *Earth Planet. Sci. Lett.* **220**, 297–316.

Dean W. E. and Parduhn N. L. (1983) Inorganic geochemistry of sediments and rocks recovered from the southern Angola Basin and adjacent Walvis Ridge, sites 530 and 532, Deep Sea Drilling Project Leg 75. In *Init. Rep & DSDP 75* (eds. W. W. Hay and J. -C. Sieiuet). Texas A&M University, ODP, College Station, TX, pp. 923–958.

Decitre S., Deloule E., Reisberg L., James R., Agrinier P. and Mével C. (2002) Behaviour of lithium and its isotopes during

serpentinization of oceanic peridotites. *Geochem. Geophys. Geosyst.* **3**, 2001GC000178.

Donnelly K. E., Goldstein S. L., Langmuir C. H. and Spiegelman M. (2004) Origin of enriched ocean ridge basalts and implications for mantle dynamics. *Earth Planet. Sci. Lett.* **226**, 347–366.

Eggins S. M., Rudnick R. L. and McDonough W. F. (1998) The composition of peridotites and their minerals: a laser ablation ICP-MS study. *Earth Planet. Sci. Lett.* **154**, 53–71.

Elliott T., Jeffcoate A. and Bouman C. (2004) The terrestrial Li isotope cycle: light-weight constraints on mantle convection. *Earth Planet. Sci. Lett.* **220**, 231–245.

Elliott T., Thomas A., Jeffcoate A. and Niu Y. (2006) Lithium isotope evidence for subduction-enriched mantle in the source of mid-ocean ridge basalts. *Nature* **443**, 565–568.

Engi M., Berger A. and Roselle G. T. (2001) Role of the tectonic accretion channel in collisional orogeny. *Geology* **29**, 1143–1146.

Evans B. (2004) The serpentinite multisystem revisited: chrysotile is metastable. *Int. Geol. Rev.* **46**, 479–506.

Gao Y., Hoefs J., Cooper K. M., Laverne C., Teagle D. A., Banerjee N. R., Alt J. C. and Casey J. F. (2007) Lithium and oxygen isotopic composition of the oceanic crust formed at a superfast spreading ridge, Hole 1256D. *Eos Trans. AGU, 88(52), Fall Meet. Suppl., Abstr.*, V11E-07.

Gerya T. V., Stoeckhert B. and Perchuck A. L. (2002) Exhumation of high-pressure metamorphic rocks in a subduction channel; a numerical simulation. *Tectonics* **21**, 6–19.

Giaramita M. J. and Sorensen S. S. (1994) Primary fluids in low-temperature eclogites evidence from two subduction complexes (Dominican Republic, and California, USA). *Contrib. Mineral. Petrol.* **117**, 279–292.

Gregoire D. C., Acheson B. M. and Taylor R. P. (1996) Measurement of lithium isotope ratios by inductively coupled plasma mass spectrometry: application to geological materials. *J. Anal. At. Spectrom.* **11**, 765–772.

Harlow G. E. (1994) Jadeitites, albitites and related rocks from the Motagua fault zone, Guatemala. *J. Metamorph. Geol.* **12**, 49–68.

Harlow G. E. (1995) Crystal chemistry of barian enrichment in micas from metasomatized inclusions in serpentinite, Motagua Valley, Guatemala. *Eur. J. Mineral.* **7**, 775–789.

Harlow G. E. and Sorensen S. S. (2005) Jade (nephrite and jadeite) and serpentinite: metasomatic connections. *Int. Geol. Rev.* **47**, 113–146.

Harlow G. E., Sisson V. B., Avé Lallemant H. G., Sorensen S. S. and Seitz R. (2003) High-pressure, metasomatic rocks along the Motagua Fault Zone, Guatemala. *Ofioliti* **28**, 115–120.

Harlow G. E., Hemming S. R., Ave Lallemant H. G., Sisson V. B. and Sorensen S. S. (2004) Two high-pressure–low-temperature serpentinite-matrix mélange belts, Motagua fault zone, Guatemala: a record of Aptian and Maastrichtian collisions. *Geology* **32**, 17–20.

Harlow G. E., Sorensen S. S. and Sisson V. B. (2007) Jade. In *The Geology of Gem Deposits*, vol. 37 (ed. L. A. Groat), pp. 207–254. Short Course Handbook Series. Mineralogical Association of Canada, Quebec.

Harlow G. E., Sisson V. B. and Sorensen S. S. (in press) Jadeitite from Guatemala: Distinctions among multiple sources. *Geol. Acta*.

Hauri E. H., Wagner T. P. and Grove T. L. (1994) Experimental and natural partitioning of Th–U–Pb and other trace elements between garnet clinopyroxene and basaltic melts. *Chem. Geol.* **117**, 149–166.

Hoefs J. and Sywall M. (1997) Lithium isotope composition of Quaternary and Tertiary biogene carbonates and a global lithium balance. *Geochim. Cosmochim. Acta* **61**, 2679–2690.

Huh Y., Chan L.-H., Zhang L. and Edmond J. M. (1998) Lithium and its isotopes in major world rivers: implications for weathering and the oceanic budget. *Geochim. Cosmochim. Acta* **62**, 2039–2051.

Ionov D. A. and Seitz H.-M. (2008) Lithium abundances and isotopic compositions in mantle xenoliths from subduction and intra-plate settings: mantle sources vs. eruption histories. *Earth Planet. Sci. Lett.* **266**, 316–331.

Jeffcoate A., Elliott T., Thomas A. and Bouman C. (2004) Precise, small sample size determination of lithium isotopic compositions of geological reference materials and modern seawater by MC-ICP-MS. *Geostand. Geoanal. Res.* **28**, 161–172.

Jeffcoate A. B., Elliott T., Kasemann S. A., Ionov D., Cooper K. and Brooker R. (2007) Li isotope fractionation in peridotites and mafic melts. *Geochim. Cosmochim. Acta* **71**, 202–218.

Johnson C. A. and Harlow G. E. (1999) Guatemala jadeitites and albitites were formed by deuterium-rich serpentinizing fluids deep within a subduction zone. *Geology* **27**, 629–632.

Johnson M. C. and Plank T. (1999) Dehydration and melting experiments constrain the fate of subducted sediments. *Geochem. Geophys. Geosyst.*, 1999GC000014.

Kelley K. A., Plank T., Ludden J. and Stuadigel H. (2003) Composition of altered oceanic crust at ODP Sites 801 and 1149. *Geochem. Geophys. Geosyst.*. doi:10.1029/2002GC000435.

King R. L., Bebout G. E., Moriguti T. and Nakamura E. (2006) Elemental mixing systematic and Sr–Nd isotopes geochemistry of mélange formation: obstacles to identification of fluid sources to arc volcanic. *Earth Planet Sci. Lett.* **246**, 288–304.

Kosler J., Kucera M. and Sylvester P. (2001) Precise measurement of Li isotopes in planktonic foraminiferal tests by quadrupole ICPMS. *Chem. Geol.* **181**, 169–179.

Kretz R. (1983) Symbols for rock-forming minerals. *Am. Min.* **68**, 277–279.

Leeman W. P., Tonarini S., Chan L.-C. and Borg L. E. (2004) Boron and lithium isotopic variations in a hot subduction zone – the southern Washington Cascades. *Chem. Geol.* **212**, 101–124.

Ludstrom C., Chaussidon M., Hsui A., Kelemen P. and Zimmerman M. (2005) Observations of Li isotopic variations in the Trinity Ophiolite: evidence for isotopic fractionation by diffusion during mantle melting. *Geochim. Cosmochim. Acta* **69**, 735–751.

Magaritz M. and Taylor, Jr., H. P. (1976) Oxygen, hydrogen and carbon isotope studies of the Franciscan Formation, Coast Ranges, California. *Geochim. Cosmochim. Acta* **40**, 215–234.

Magenheim A. J., Spivack A. J., Alt J. C., Bayhurst G., Chan L. H., Gieskes J. M. and Zuleger E. (1995) Borehole fluid chemistry in Hole 504B, Leg 137: formation water or in situ reaction? *Proc. Ocean Drill. Program* **137**(140), 141–152.

Marschall H. R. and Pogge von Strandmann P. A. E. (2008) Li and Mg exchange between eclogite lenses and their host rocks: evidence from isotope profiles. *Geochim. Cosmochim. Acta* **72**(Suppl. 1), A594.

Marschall H. R., Altherr R., Ludwig T., Kalt A., Gmeling K. and Kasztovszky Z. (2006) Partitioning and budget of Li, Be and B in high-pressure metamorphic rocks. *Geochim. Cosmochim. Acta* **70**, 4750–4769.

Marschall H. R., Altherr R. and Rüpke L. (2007a) Squeezing out the slab – modeling the release of Li, Be and B during progressive high-pressure metamorphism. *Chem. Geol.* **239**, 323–335.

Marschall H. R., Pogge von Strandmann P. A. E., Seitz H.-M., Elliott T. and Niu Y. (2007b) The lithium isotopic composition of orogenic eclogites and deep subducted slabs. *Earth Planet. Sci. Lett.* **262**, 563–580.

McDonough W. F. and Sun S. S. (1995) The composition of the Earth. *Chem. Geol.* **120**, 223–253.

Moriguti T. and Nakamura E. (1998a) Across-arc variation of Li isotopes in lavas and implications for crust/mantle recycling at subduction zones. *Earth Plant. Sci. Lett.* **163**, 167–174.

Moriguti T. and Nakamura E. (1998b) High yield separation and the precise isotopic analysis for natural rock and aqueous samples. *Chem. Geol.* **145**, 91–104.

Navon O. and Stolper E. (1987) Geochemical consequences of melt percolation; the upper mantle as a chromatographic column. *J. Geol.* **95**, 285–307.

Nelson B. K. (1991) Sediment-derived fluids in subduction zones: isotopic evidence from veins in blueschist and eclogite of the Franciscan Complex, California. *Geology* **19**, 1033–1036.

Nelson B. K. (1995) Fluid flow in subduction zones; evidence from Nd- and Sr-isotope variation in metabasalts of the Franciscan Complex, California. *Contrib. Mineral. Petrol.* **119**, 247–262.

Nishio Y. and Nakai S. (2002) Accurate and precise lithium isotopic determinations of igneous rock samples using multi-collector inductively coupled plasma mass spectrometry. *Anal. Chim. Acta* **456**, 271–281.

Nishio Y., Nakai S., Kogiso T. and Barsczus H. G. (2005) Lithium, strontium, and neodymium isotopic compositions of oceanic island basalts in the Polynesian region; constraints on a Polynesian HIMU origin. *Geochem. J.* **39**, 91–103.

Nishio Y., Nakai S., Ishii T. and Sano Y. (2007) Isotope systematics of Li, Sr, Nd, and volatiles in Indian Ocean MORBs of the Rodrigues Triple Junction: constraints on the origin of the DUPAL anomaly. *Geochim. Cosmochim. Acta* **71**, 745–759.

Oh C.-W. and Liou J. G. (1990) Metamorphic evolution of two different eclogites in the Franciscan Complex, California, USA. *Lithos* **25**, 41–53.

Page F. Z., Essene E. J., Mukasa S. B. and Armstrong L. S. (2003) Prograde and retrograde history of the Healdsburg Eclogite, California. *Geol. Soc. Am. Abstr.* **35**, 640.

Penniston-Dorland S., Khadke S. V. and Sorensen S. S. (2008) Fluid flow in subduction zone high grade blocks of the Franciscan Complex, CA: evidence from Li and Li isotopes. *Eos Trans. AGU, 89(53), Fall Meet. Suppl., Abstr.*, V34B-01.

Pistiner J. and Henderson G. (2003) Lithium-isotope fractionation during continental weathering processes. *Earth Plant. Sci. Lett.* **214**, 327–339.

Plank T. and Langmuir C. H. (1998) The chemical composition of subducting sediment and its consequences for the crust and mantle. In *Geochemical Earth Reference Model (GERM)* (eds. F. Albarede, T. J. Blichert, H. Staudigel and W. M. White). *Chem. Geol.* **145**, 325–394.

Ramsey M. H., Potts P. J., Webb P. C., Watkins P., Watson J. S. and Coles B. J. (2005) An objective assessment of analytical method precision: comparison of ICP-AES and XRF for the analysis of silicate rocks. *Chem. Geol.* **124**, 1–19.

Richter F. M., Davis A. M., Depaolo D. J. and Watson E. B. (2003) Isotope fractionation by chemical diffusion between molten basalt and rhyolite. *Geochim. Cosmochim. Acta* **67**, 3905–3923.

Rosner M., Bach W., Erzinger J., Peucker-Ehrenbrink B. and Worthington T. (2005) Lithium isotope cycling in subduction zones: the Tonga Island arc/back-arc system. *Eos Trans. AGU, 86(52), Fall Meet. Suppl., Abstr.*, V31C-0634.

Rosner M., Ball L., Peucker-Ehrenbrink B., Blusztajn J., Bach J. and Erzinger J. (2007) A simplified, accurate and fast method for lithium isotope analysis of rocks and fluids, and ^{7}Li values of seawater and rock reference materials. *Geostand. Geoanal. Res.* **31**, 77–88.

Rudnick R. L. and Ionov D. A. (2007) Lithium elemental and isotopic disequilibrium in minerals from peridotite xenoliths from far-east Russia: poduct of recent melt/fluid–rock reaction. *Earth Planet. Sci. Lett.* **256**, 278–293.

Rudnick R. L., Tomascak P. B., Njoa H. B. and Gardner L. R. (2004) Extreme lithium isotopic fractionation during continental weathering revealed in saprolites from South Carolina. *Chem. Geol.* **212**, 45–57.

Ryan J. G. and Kyle P. R. (2004) Lithium abundance and lithium isotope variations in mantle sources: insights from intraplate volcanic rocks from Ross Island and Marie Byrd Land (Antarctica) and other oceanic islands. *Chem. Geol.* **212**, 125–142.

Ryan J. G. and Langmuir C. H. (1987) The systematics of lithium abundances in young volcanic rocks. *Geochim. Cosmochim. Acta* **51**, 1727–1741.

Savov I. P., Ryan J. G., D'Antonio M., Kelley K. and Mattie P. (2005) Geochemistry of serpentinized peridotites from the Mariana Forearc Conical Seamount, ODP Leg 125: implications for the elemental recycling at subduction zones. *Geochem. Geophys. Geosys.* **6**. doi:10.1029/2004GC000777.

Schmidt M. W. and Poli S. (2003) Generation of mobile components during subduction of oceanic crust. In *The Crust* (ed. R. L. Rudnick) vol. 3. *Treatise on Geochem.* (eds. H. D. Holland and K. K. Turekian). pp. 567–590.

Seitz H.-M. and Woodland A. B. (2000) The distribution of lithium in peridotitic and pyroxenitic mantle lithologies – an indicator of magmatic and metasomatic processes. *Chem. Geol.* **166**, 47–64.

Seitz H.-M., Brey G. B., Stachel T. and Harris J. W. (2003) Li abundances in inclusions in diamonds from the upper and lower mantle. *Chem. Geol.* **201**, 307–318.

Seyfried, Jr, W. E., Janecky D. R. and Mottl M. (1984) Alteration of the oceanic crust by seawater: implications for the geochemical cycles of boron and lithium. *Geochim. Cosmochim. Acta* **48**, 557–569.

Shreve R. L. and Cloos M. (1986) Dynamics of sediment subduction, mélange formation, and prism accretion. *J. Geophys. Res.* **91**, 10229–10245.

Simons K. K. (2008) Lithium Isotope Variability: new constraints on mantle heterogeneity. Ph. D. dissertation, Columbia University.

Simons K. K., Goldstein S. L., Langmuir C. H. and Hemming N. G. (2008) Lithium isotope systematics of the Azores Platform: insights into Li variability of mantle sources. *Eos Trans. AGU, 89(53), Fall Meet. Suppl., Abstr.*, V43C-2176.

Sisson V. B., Harlow G. E. and Sorensen S. S. (2005) Jadeitite: a record of metasomatism at various depths in Guatemalan subduction zones. *Geochim. Cosmochim. Acta* **69**(Suppl. 1), A785.

Sorensen S. S., Grossman J. N. and Perfit M. R. (1997) Phengite-hosted LILE enrichment in eclogite and related rocks: Implications for fluid-mediated mass transfer in subduction zones and arc magma genesis. *J. Petrol.* **38**, 3–34.

Sorensen S. S., Harlow G. E. and Rumble D. (2006) The origin of jadeitite-forming subduction zone fluids: CL-guided SIMS oxygen isotope and trace element evidence. *Am. Mineral.* **91**, 979–996.

Sorensen S. S., Sisson V. B., Harlow G. E., Avé Lallemant H. G. and Tsujimori T. (2007) Jadeitite, lawsonite eclogite, and related rocks, Guatemala: fluid–rock histories from a cold subduction zone. *Geochim. Cosmochim. Acta* **71**(Suppl. 1), A957.

Strelow F., Weinert C. H. S. W. and Van der Walt T. N. (1974) Separation of lithium from sodium, beryllium and other

elements by cation-exchange chromatography in nitric acid–methanol. *Anal. Chim. Acta* **71**, 123–132.

Sun S. S. and McDonough W. F. (1989) Chemical and isotopic systematics of oceanic basalts: implications for mantle composition and processes. In *Magmatism in the an Basins*, vol. 42 (eds. A. D. Saunders and M. J. Norry). Geol. Soc. Special Publication, pp. 313–345.

Tang Y.-J., Zhang Hong-F, Nakamura Eiz, Moriguti Takuy, Kobayashi Katsur and Ying Ji-Fen (2007) Lithium isotopic systematics of peridotite xenoliths from Hannuoba, North China Craton: implications for melt–rock interaction in the considerably thinned lithospheric mantle. *Geochim. Cosmochim. Acta* **71**, 4327–4341.

Taylor, Jr., H. P. and Coleman R. G. (1968) O^{18}/O^{16} ratios of coexisting minerals in glaucophane-bearing metamorphic rocks. *Geol. Soc. Am. Bull.* **79**, 1727–1755.

Taylor T. I. and Urey H. C. (1938) Fractionation of the lithium and potassium isotopes by chemical exchange with zeolites. *J. Chem. Phys.* **6**, 429–438.

Teng F.-Z., McDonough W. F., Rudnick R. L., Dalpe C., Tomascak P. B., Chappell B. W. and Gao S. (2004) Lithium isotopic composition and concentration of the upper continental crust. *Geochim. Cosmochim. Acta* **68**, 4167–4178.

Teng F.-Z., McDonough W. F., Rudnick R. L. and Walker R. J. (2006) Diffusion-driven extreme lithium isotopic fractionation in country rocks of the Tin Mountain pegmatite. *Earth Planet. Sci. Lett.* **243**, 701–710.

Teng F.-Z., McDonough W. F., Rudnick R. L. and Wing B. A. (2007) Limited lithium isotopic fractionation during progressive metamorphic dehydration in metapelites: a case study from the Onawa contact aureole. *Maine. Chem. Geol.* **239**, 1–12.

Teng F.-Z., Rudnick R. L., McDonugh W. F., Gao S., Tomascak P. B. and Liu Y. (2008) Lithium isotopic composition and concentration of the deep continental crust. *Chem. Geol.* **255**, 47–59.

Tomascak P. B. (2004) Developments in the understanding and application of lithium isotopes in the Earth and planetary sciences. In *Geochemistry of Non-Traditional Stable Isotopes* (eds. C. Johnson, B. Beard and F. Albarede). Mineral. Soc. Am., Washington, DC, pp. 153–195.

Tomascak P., Carlson R. and Shirey S. (1999a) Accurate and precise determination of Li isotopic compositions by multi-collector sector ICP-MS. *Chem. Geol.* **158**, 145–154.

Tomascak P., Tera F., Helz R. and Walker R. (1999b) The absence of lithium isotope fractionation during basalt differentiation: New measurements by multicollector sector ICP-MS. *Geochim. Cosmochim. Acta* **63**, 907–910.

Tomascak P. B., Ryan G. J. and Defant M. J. (2000) Lithium isotope evidence for light element decoupling in the Panama subarc mantle. *Geology* **28**, 507–510.

Tomascak P. B., Widom E., Benton L. D., Goldstein S. J. and Ryan J. G. (2002) The control of lithium budgets in island arcs. *Earth Planet. Sci. Lett.* **196**, 227–238.

Tomascak P. B., Langmuir C. H., LeRoux P. and Shirey S. B. (2008) Lithium isotopes in global mid-ocean ridge basalts. *Geochim. Cosmochim. Acta* **72**, 1626–1637.

Tsujimori T., Liou J. G. and Coleman R. G. (2004) Comparison of two contrasting eclogites from the Motagua Fault Zone, Guatemala: Southern lawsonite eclogite versus northern zoisite eclogite. *Geol. Soc. Am. Abstr.* **36**, 136.

Tsujimori T., Liou J. G. and Coleman R. G. (2005) Coexisting retrograde jadeite and omphacite in a jadeite-bearing lawsonite eclogite from the Motagua fault zone, Guatemala. *Am. Mineral.* **90**, 836–842.

Tsujimori T., Sisson V. B., Liou J. G., Harlow G. E. and Sorensen S. S. (2006a) Petrologic characterization of Guatemalan lawsonite eclogite: eclogitization of subducted oceanic crust in a cold subduction zone. *Geol. Soc. Am. Special Paper* **403**, 147–168.

Tsujimori T., Sisson V. B., Liou J. G., Harlow G. E. and Sorensen S. S. (2006b) Very-low-temperature record of the subduction process: a review of worldwide lawsonite eclogites. *Lithos* **92**, 609–624.

Vils F., Pelletier L., Kalt A., Muntener O. and Ludwig T. (2008) The Lithium, Boron and Beryllium content of serpentinized peridotites from ODP Leg 209 (Sites 1272A and 1274A): implications for lithium and boron budgets of oceanic lithosphere. *Geochim. Cosmochim. Acta* **72**, 5475–5504.

Wood B. J. and Blundy J. D. (2007) Trace element partitioning under crustal and uppermost mantle conditions: the influences of ionic radius, cation charge, pressure, and temperature. In *The Mantle and Core* (ed. R. W. Carlson) vol. 2. *Treatise on Geochemistry* (eds. Holland and K. K. Turekian). pp. 395–424.

Woodland A. B., Seitz H.-M., Altherr R., Marschall H., Olker B. and Ludwig T. (2002) Li abundances in eclogite minerals: a clue to a crustal or mantle origin? *Contrib. Mineral. Petrol.* **143**, 587–601.

Wunder B., Meixner A., Romer R. and Heinrich W. (2006) Temperature-dependent isotopic fractionation of lithium between clinopyroxene and high-pressure hydrous fluids. *Contrib. Mineral. Petrol.* **151**, 112–120.

Wunder B., Meixer A., Romer R. L., Feenstra A., Schettler G. and Heinrich W. (2007) Lithium isotope fractionation between Li-bearing staurolite, Li-mica and aqueous fluids: an experimental study. *Chem. Geol.* **238**, 277–290.

You C.-F. and Chan L.-H. (1996) Precise determination of lithium isotopic composition in low concentration natural samples. *Geochim. Cosmochim. Acta* **60**, 909–915.

You C.-F., Chan L.-H., Spivak A. J. and Geiskes J. M. (1995) Lithium, boron, and their isotopes in ODP Site 808, Nankai Trough sediments and pore waters: implications for fluid expulsion in accretionary prisms. *Geology* **23**, 37–40.

Zack T., Rivers T. and Foley S. F. (2001) Cs–Rb–Ba systematics in phengite and amphibole: an assessment of fluid mobility at 2 GPa in eclogites from Trescolmen, Central Alps. *Contrib. Mineral. Petrol.* **140**, 97–122.

Zack T., Foley S. F. and Rivers T. (2002) Equilibrium and disequilibrium trace element partitioning in hydrous eclogites (Trescolmen, Central Alps). *J. Petrol.* **43**, 1947–1974.

Zack T., Tomascak P. B., Rudnick R. L., Dalpe C. and McDonough W. F. (2003) Extremely light Li in orogenic eclogites: the role of isotopic fractionation during dehydration in subducted oceanic crust. *Earth Plant. Sci. Lett.* **208**, 279–290.

Associate editor: F.J. Ryerson